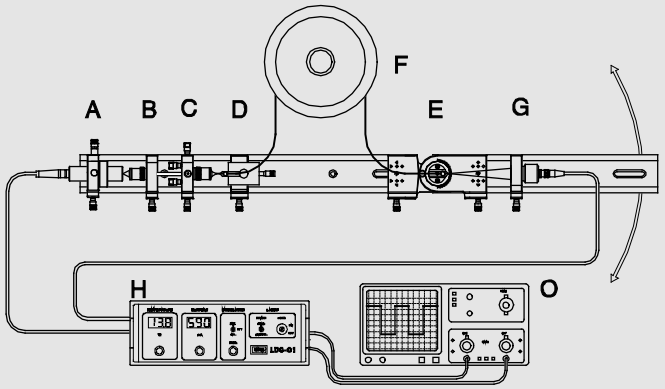

EXPERIMENT 12

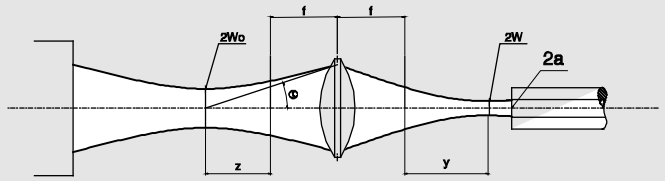

FIBRE OPTICS

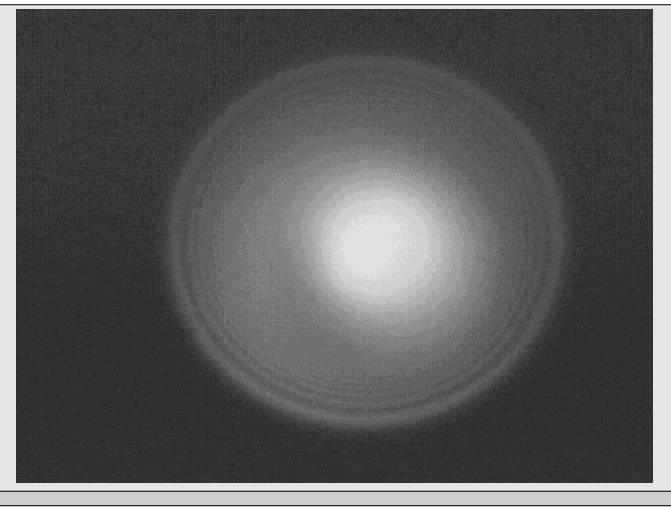

MEOS

Didactic Counsellor

Prof. Dr.-Ing. Dickmann

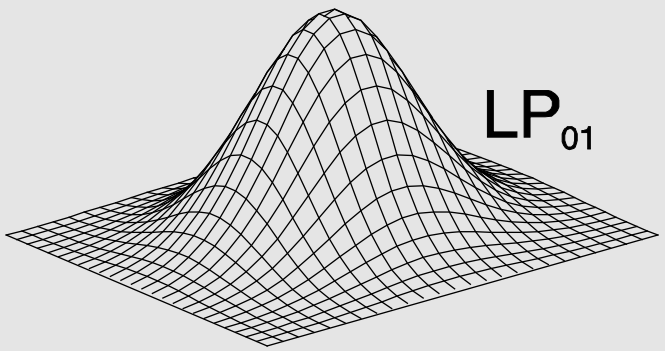

Fachhochschule
M•nster

Fachbereich
Physikal. Technik

1 Introduction

One essential desire of human beings is to use information faster than others for their own benefit. In his publication „Die Quasioptik der Ultrakurzwellenleiter" H.Buchholz expressed in 1939 the idea to guide light signals along light conducting material and to use them for data transmission. But only with the development of the semiconductor laser in 1962 Buchholz' idea was materialising by using just these lasers and fibres as light transmitting medium. Suddenly simple and powerful light sources for the generation and modulation of light were available. Today the transmission of signals using laser diodes and fibres has become an indispensable technology and the on-going development in this area is one of the most important within this century. Following the achievements of communication technology the development of fibre optical sensors began in 1977. Here the laser gyroscope for navigation has to be emphasised in particular. This new technology is based on well known fundamentals in a way that no new understanding has to be created. Still, there is a challenge with respect to the technical realisation keeping in mind that the light has to be guided within fibres of 5 µm diameter only. Appropriate fibres had to be developed and mechanical components of high precision had to be disposed for coupling the light to the conductor (fibre) and for the installation of the fibres. Further goals are the reduction of transmission losses, optical amplification within the fibre as replacement of the electronic amplifiers and laser diodes of small band width to increase the transmission speed of signals.

2 Basics

There is hardly any book in optics which does not contain the experiment of Colladan (1861) on total reflection of light. Most of us may have enjoyed it during the basic physics course.

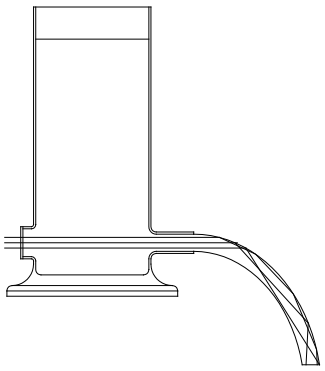

Fig. 1: Colladan's (1861) experiment for the demonstration of the total reflection of light

An intensive light beam is introduced into the axis of an out flowing water jet. Because of repeated total reflections the light cannot leave the jet and it is forced to follow the water jet. It is expected that the jet remains completely darken unless the surface contains small disturbances. This leads to a certain loss of light and it appears illuminated all along its way. Effects of light created in this way are also known as „Fontaines lumineuses". They please generally the onlookers of water games. This historical experiment already shows the physical phenomena which are basic in fibre optics. The difference of this light conductor to modern fibres is the dimension which for a fibre is in the order of magnitude of the wavelength of light. If we designate the diameter of a light guide with d we can state:

„Fontaines lumineuses"	$d >> \lambda$
Multimode fibres	$d > \lambda$
Monomode fibres	$d \approx \lambda$

For the fibres manufactured these days this leads to further effects which can not be described exclusively by total reflection. Their understanding is of special importance for optical communication technology. In the following we will deduce these effects based on Maxwell's equations. For the work in fibre optics it is not compulsory to know this formalism. It is sufficient to familiarise oneself with the results. When we are going to derive this formalism within the context of this manual we do it because it has never been done before in a comprehensive way within the ordinary teaching manuals with some exceptions [1] or it has been insufficiently dealt with vis a vis the multitude of various light conductors.

2.1 Maxwell's equations

We begin with Maxwell's equations which are the basis for the description of all electromagnetic phenomena. The equations are presented in two ways. First we describe the state of the vacuum by introducing the electric field strength $\vec{E}$ and the magnetic field strength $\vec{H}$. This description surely gives a sense whenever the light beam propagates within free space. The situation will be different when the light beam propagates in matter. In this case the properties of matter have to be respected. Contrary to vacuum matter can have electric and magnetic properties. These are the current density $\vec{j}$, the displacement $\vec{D}$ and the magnetic induction $\vec{B}$.

Maxwell's Equations:

$$\nabla \times \vec{H} = \varepsilon \cdot \varepsilon_0 \cdot \frac{\partial \vec{E}}{\partial t} + \sigma \cdot \vec{E} \text{ and } \nabla \cdot \vec{H} = 0$$

$$\text{or } \nabla \times \vec{H} = \frac{\partial \vec{D}}{\partial t} + \vec{j} \qquad \textbf{(2.1.1)}$$

$$\nabla \times \vec{E} = -\mu \cdot \mu_0 \cdot \frac{\partial \vec{H}}{\partial t} \text{ and } \nabla \cdot \vec{E} = \frac{4\pi}{\varepsilon} \cdot \rho$$

$$\text{or } \nabla \times \vec{E} = -\frac{\partial \vec{B}}{\partial t} \qquad \textbf{(2.1.2)}$$

$$\nabla = \left(\frac{\partial}{\partial x}, \frac{\partial}{\partial y}, \frac{\partial}{\partial z} \right), \nabla\times \equiv rot \ , \nabla\cdot \equiv div$$

ε_0 is the dielectric constant of the free space. It represents the ratio of unit charge (As) to unit field strength (V/m) and amounts to 8.859 10^{-12} As/Vm.

ε is the dielectric constant of matter. It characterises the degree of extension of an electric dipole acted on by an external electric field $\vec{E}$. The dielectric constant ε and the susceptibility χ are linked by the following relation: $\varepsilon = \frac{1}{\varepsilon_0} \cdot (\chi + \varepsilon_0)$. The product $\varepsilon \cdot \varepsilon_0 \cdot \vec{E} = \vec{D}$ is therefore called „dielectric displacement“ or displacement.

σ is the electric conductivity of matter .The product $\sigma \cdot \vec{E} = \vec{j}$ represents the electric current density

μ_0 is the absolute permeability of the free space. It gives the context between the unit of an induced voltage (V) due to the presence of a magnetic field H of unit Am/s. It amounts to 1.256 10^{-6} Vs/Am.

μ is like ε a constant of the matter under consideration. It describes the degree of displacement of magnetic dipoles under the action of an external magnetic field $\vec{H}$. The product of permeability μ and magnetic field strength $\vec{H}$ is called magnetic induction $\vec{B} = \mu \cdot \mu_0 \cdot \vec{H}$.

ρ is the charge density. It is the source which generates electric fields. The operation ∇ or div provides the source strength and is a measure for the intensity of the generated electric field. The charge carrier is the electron which has the property of a monopole. On the contrary there are no magnetic monopoles but only dipoles. Therefore $\nabla \cdot \vec{H}$ is always zero.

Within the frame of further considerations we will refer to fibres as light conductors which are made of glass or similar matter. They have no electric conductivity (e. g. σ = 0), no free charge carriers ($\nabla \vec{E} = 0$) and no magnetic dipoles (μ = 1). Therefore the Maxwell equations adapted to our problem are as follows:

$$\nabla \times \vec{H} = \varepsilon \cdot \varepsilon_0 \cdot \frac{\partial \vec{E}}{\partial t} \quad \text{and} \ \nabla \cdot \vec{H} = 0 \qquad \textbf{(2.1.3)}$$

$$\nabla \times \vec{E} = -\mu_0 \cdot \frac{\partial \vec{H}}{\partial t} \quad \text{and} \ \nabla \cdot \vec{E} = 0 \qquad \textbf{(2.1.4)}$$

2.2 Wave Equation

Using the above equations the goal of the following calculations will be to get an appropriate set of equations describing the propagation of light in glass or similar matter. After this step we will introduce the boundary conditions which have to be implemented due to the use of fibre glass. Let's do the first step first. Let's eliminate the magnetic field strength $\vec{H}$ to get an equation which only contains the electric field strength $\vec{E}$. By forming the time derivation of **(2.1.3)** and executing the operation $\nabla \times$ on **(2.1.4)** we get:

$$\nabla \times \frac{\partial \vec{H}}{\partial t} - \varepsilon \cdot \varepsilon_0 \cdot \frac{\partial^2 \vec{E}}{\partial t^2} = 0$$

$$\nabla \times (\nabla \times \vec{E}) + \mu_0 \cdot \nabla \times \frac{\partial \vec{H}}{\partial t} = 0$$

By substitution we get:

$$\nabla \times (\nabla \times \vec{E}) + \mu_0 \cdot \varepsilon \cdot \varepsilon_0 \frac{\partial^2 \vec{E}}{\partial t^2} = 0 \qquad \textbf{(2.2.1)}$$

The following vector identity is always valid:

$$\nabla \times (\nabla \times \vec{E}) = -\nabla \cdot \nabla \vec{E} + \nabla (\nabla \cdot \vec{E}) ,$$

where $\nabla \cdot \nabla = \Delta$ is the abbreviation for the Laplace operator

$$\Delta = \frac{\partial^2}{\partial x^2} + \frac{\partial^2}{\partial y^2} + \frac{\partial^2}{\partial z^2}$$

Let's use the identity for (2.2.1). So we get:

$$\Delta \vec{E} - \mu_0 \cdot \varepsilon_0 \cdot \varepsilon \cdot \frac{\partial^2 \vec{E}}{\partial t^2} = 0 \qquad \textbf{(2.2.2)}$$

Using for the velocity of light in vacuum the relation

$$c = \frac{1}{\sqrt{\varepsilon_0 \cdot \mu_0}}$$

and Maxwell's relation $n = \sqrt{\varepsilon \cdot \mu}$ (n is the refractive index), we get with μ = 1 as a result the wave equation for the electric field $\vec{E}$ in glass:

$$\Delta \vec{E} - \frac{n^2}{c^2} \cdot \frac{\partial^2 \vec{E}}{\partial t^2} = 0 . \qquad \textbf{(2.2.3)}$$

In the same way we get the wave equation for the magnetic field $\vec{H}$

$$\Delta \vec{H} - \frac{n^2}{c^2} \cdot \frac{\partial^2 \vec{H}}{\partial t^2} = 0 \qquad \textbf{(2.2.4)}$$

The first step of our considerations has been completed. Both equations contain a term which describes the spatial dependence (Laplace operator) and a term which contains the time dependence. Both equations seem to be very „theoretical“ but their practical value will soon become evident. Now we have to clarify how the wave equations will look like when the light wave hits a boundary. This situation is given whenever two media of different refractive index are in mutual contact. After having performed this step we will be in a position to derive all laws of optics from Maxwell's equations. Let's return to the boundary problem. This can be solved in different ways. We will go the simple but safe way and request the validity of the law of conservation of energy. This means that the energy which arrives per unit time at one side of the boundary has to leave it at the other side in the same unit of time since there can not be any loss nor accumulation of energy at the boundary. Till now we did not yet determine the energy of an electromagnetic field. This will be done next for any medium. The power available per unit volume δW consists of two parts as will be shown now. The power is generated by a current density $\vec{j}$ at a field strength $\vec{E}$. We have:

$$\delta W = \vec{j} \cdot \vec{E} .$$

We calculate $\vec{j} \cdot \vec{E}$ using the vector identity

$$\nabla \cdot (\vec{E} \times \vec{H}) = \vec{H} \cdot (\nabla \times \vec{E}) - \vec{E} \cdot (\nabla \times \vec{H})$$

as well as (2.1.1) and (2.1.2). We get:

$$\delta W = -\nabla \cdot (\vec{E} \times \vec{H}) - \vec{H} \cdot \frac{\partial \vec{B}}{\partial t} - \vec{E} \cdot \frac{\partial \vec{D}}{\partial t}$$

with $\vec{B} = \mu \cdot \mu_0 \cdot \vec{H}$ and $\vec{D} = \varepsilon \cdot \varepsilon_0 \cdot \vec{E}$

$$\delta W = -\nabla \cdot (\vec{E} \times \vec{H}) - \frac{\partial}{\partial t}(\tfrac{1}{2}\mu\mu_0 \cdot \vec{H}^2 + \tfrac{1}{2}\varepsilon \cdot \varepsilon_0 \cdot \vec{E}^2)$$

It is evident that the second term in the above equation contains the stored electromagnetic energy per unit volume W_{em}

$$W_{em} = \frac{1}{2}\mu\mu_0 \cdot \vec{H}^2 + \frac{1}{2}\varepsilon\varepsilon_0 \cdot \vec{E}^2$$

The first term contains the energy flux density vector

$$\vec{S} = \vec{E} \times \vec{H}$$

also known as Poynting vector. The conservation of energy can now simply be expressed as follows:

$$-\partial W = \nabla \cdot \vec{S} + \frac{\partial W_{em}}{\partial t} = -\vec{j} \cdot \vec{E}$$

We required that the energy flux in medium 1 flowing to the boundary is equal to the energy flux in medium 2 flowing away from the boundary. Let's choose as normal to the boundary the direction of the z-axis of the coordinate system. The following must be true:

$$\vec{S}_z^1 = \vec{S}_z^2$$

$$(\vec{E}^1 \times \vec{H}^1)_z = (\vec{E}^2 \times \vec{H}^2)_z$$

By evaluation of the vector products we get:

$$E_x^1 \cdot H_y^1 - H_x^1 \cdot E_y^1 = E_x^2 \cdot H_y^2 - H_x^2 \cdot E_y^2 .$$

Since the continuity of the energy flux must be assured for any type of electromagnetic field we have additionally:

$$E_x^1 = E_x^2 \qquad H_x^1 = H_x^2$$
$$E_y^1 = E_y^2 \qquad H_y^1 = H_y^2$$
$$E_{tg}^1 = E_{tg}^2 \qquad H_{tg}^1 = H_{tg}^2$$

This set of vector components can also be expressed in the following way:

$$\nabla \times \vec{E} = \vec{N} \times (\vec{E}_2 - \vec{E}_1) = 0 \text{ and } \nabla \times \vec{H} = 0 \quad \textbf{(2.2.5)}$$

$\vec{N}$ is the unit vector and vertical to the boundary. Substituting (2.2.5) into (2.1.1) or (2.1.2) it can be shown that the components of $\vec{D} = \varepsilon\varepsilon_0 \cdot \vec{E}$ and $\vec{B} = \mu\mu_0 \cdot \vec{H}$ in the direction of the normal $\vec{N}$ are continuous, but $\vec{E}$ and $\vec{H}$ are discontinuous in the direction of the normal. Let's summarise the results regarding the behaviour of a field at a boundary:

$E_{tg}^1 = E_{tg}^2$	$D_{norm}^1 = D_{norm}^2$
$H_{tg}^1 = H_{tg}^2$	$B_{norm}^1 = B_{norm}^2$

By means of the equations (2.1.1), (2.1.2) and the above continuity conditions we are now in a position to describe any situation at a boundary.

2.3 Fibres as light wave conductors

Glass fibres as wave conductors have a circular cross section. They consist of a core of refractive index n_k. The core is surrounded by a glass cladding of refractive index n_m slightly lower than n_k. Generally the refractive index of the core as well as the refractive index of the cladding are considered homogeneously distributed. Between core and cladding there is the boundary as described in the previous chapter. The final direction of the beam is defined by the angle Θ_e under which the beam enters the fibre. Unintended but not always avoidable radiation and cladding waves are generated in this way. For reasons of mechanical protection and absorption of the radiation waves the fibre is surrounded by a protective layer.

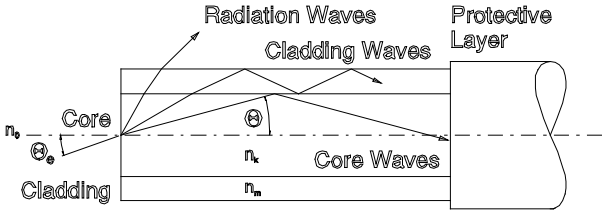

Fig. 2: Step index fibre

Fig. 2 reveals some basic facts which can be seen without having solved Maxwell's equations. Taking off from geometrical considerations we can state that there must be a limiting angle Θ_c for total reflection at the boundary between cladding and core.

$$\cos(\Theta_c) = \frac{n_m}{n_k} \qquad \textbf{(2.3.1)}$$

For the angle of incidence of the fibre we use the law of refraction:

$$\frac{\sin(\Theta_{ec})}{\sin(\Theta_c)} = \frac{n_k}{n_0}$$

and receive:

$$\Theta_{ec} = \arcsin(\frac{n_k}{n_0} \cdot \sin\Theta_c)\,.$$

Using equation (2.3.1) and with $n_o = 1$ for air we finally get:

$$\Theta_{ec} = \arcsin(\sqrt{n_k^2 - n_m^2})$$

The limiting angle Θ_{ec} represents half the opening angle of a cone. All beams entering within this cone will be guided in the core by total reflection. As usual in optics here, too, we can define a numerical aperture A:

$$A = \sin\Theta_{ec} = \sqrt{n_k^2 - n_m^2} \qquad \textbf{(2.3.2)}$$

Depending under which angle the beams enter the cylindrical core through the cone they propagate screwlike or helixlike. This becomes evident if we project the beam displacements onto the XY-plane of the fibre. The direction along the fibre is considered as the direction of the z-axis. A periodical pattern is recognised. It can be interpreted as standing waves in the XY-plane. In this context the standing waves are called oscillating modes or simply modes. Since these modes are built up in the XY-plane, e.g. perpendicularly to the z-axis, they are also called transversal modes. Modes built up along the z-axis are called longitudinal modes. For a deeper understanding of the mode generation and their properties we are now going to solve the Maxwell equations under respect of the fibre boundary conditions.

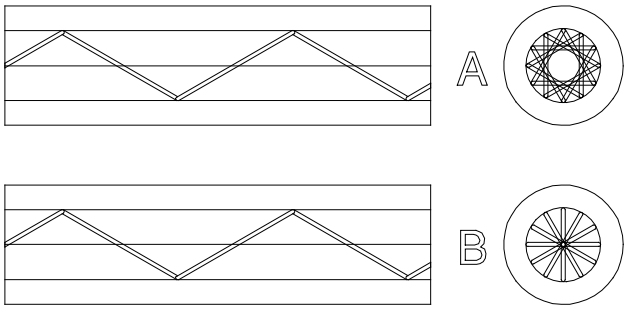

Fig. 3: Helix (A) and Meridional beam (B)

First we are only interested in the core waves. In this regard the cladding can be considered an infinitely extended medium of refractive index n_m . Because of the cylindrical symmetry of the fibre the Cartesian coordinates are replaced by cylindrical coordinates.

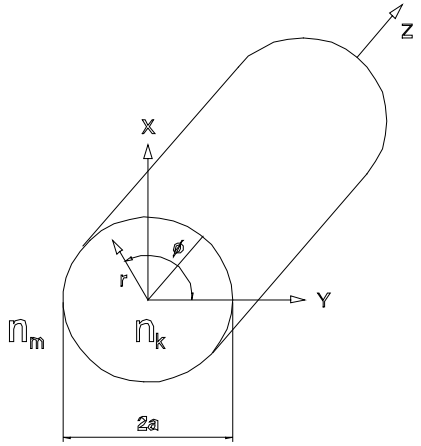

Fig. 4: Introduction of cylindrical coordinates

2.4 Wave Equation for Glass Fibres

Let's solve the wave equations which we quote once again:

$$\Delta\vec{E} - \frac{n^2}{c^2} \cdot \frac{\partial^2 \vec{E}}{\partial t^2} = 0\,. \qquad \textbf{(2.4.1)}$$

$$\Delta\vec{H} - \frac{n^2}{c^2} \cdot \frac{\partial^2 \vec{H}}{\partial t^2} = 0 \qquad \textbf{(2.4.2)}$$

Up to now there was no need to make any assumptions for $\vec{E}$ and $\vec{H}$. This will be done now. We presume that the wave will propagate in the z-direction of the fibre as shown in Fig. 3. It can propagate in zigzag or any other way. Therefore we introduce the general coefficient of propagation β which will be determined in the course of further calculations.

Statement:

$$E_r(r,\phi,z,t) = (\hat{E}_r \cdot e^{i\omega t} + \hat{E}_r^{\,*} \cdot e^{-i\omega t}) \cdot e^{-i\beta z}$$

$$E_\phi(r,\phi,z,t) = (\hat{E}_\phi \cdot e^{i\omega t} + \hat{E}_\phi^{\,*} \cdot e^{-i\omega t}) \cdot e^{-i\beta z}$$

$$E_z(r,\phi,z,t) = (\hat{E}_z \cdot e^{i\omega t} + \hat{E}_z^{\,*} \cdot e^{-i\omega t}) \cdot e^{-i\beta z} \qquad \textbf{(2.4.3)}$$

$\hat{E}_i = \hat{E}_i(r,\phi,z)$ i=r , ϕ, z are complex functions depending only on the local position. They are also called „phasors". The $*$ signifies the complex conjugate value, i. g. replacement of i by -i. First we solve the wave equation for the z-component $E_z(r,\phi,z,t)$ of $\vec{E}$ and $\vec{H}$. Then we use the Maxwell equations to get the E_r- and E_ϕ- components. Using the wave number k, the wave length λ, the frequency ν and the angular frequency ω,

$$k = \frac{2\pi}{\lambda} \text{ and } \omega = 2\pi \cdot \nu \text{ with } \nu = \frac{c}{\lambda}$$

the wave equations (2.4.1) and (2.4.2) change as follows:

$$(\Delta + k^2 \cdot n^2) E_z = 0 \qquad \textbf{(2.4.4)}$$

$$(\Delta + k^2 \cdot n^2) H_z = 0 \qquad \textbf{(2.4.5)}$$

We now use the Laplace operator in cylindrical coordinates:

$$\Delta_{cyl} = \frac{1}{r} \cdot \frac{\partial}{\partial r}(r \cdot \frac{\partial}{\partial r}) + \frac{1}{r^2} \cdot \frac{\partial^2}{\partial \phi^2} + \frac{\partial^2}{\partial z^2},$$

which we change for our purposes in the following way:

$$\Delta_{cyl} = \Delta_{r,\phi} + \Delta_z$$

The transversal and the longitudinal part of the differential equations are separated by introduction of the following product:

$$E_z = E_z(r,\phi) \cdot E_z(z)$$

In this way we get from (2.4.4):

$$(\Delta_{cyl} + k^2 \cdot n^2) \cdot E_z(r,\phi) \cdot E_z(z) = 0 \qquad \textbf{(2.4.6)}$$

With the relation

$$\Delta(E_z(r,\phi) \cdot E_z(z)) = E_z \cdot \Delta E_z(r,\phi) + E_z(r,\phi) \cdot \Delta E_z(z)$$

and with equation **(2.4.1)**we have:

$$E_z(z) \cdot (\Delta_{r,\phi} - \beta^2 + k^2 n^2) E_z(r,\phi) = 0$$

For simplification let's write:

$$k_{rn}^2 = n^2 k^2 - \beta^2$$

Since $E_z(z)$ may have values different from zero we must request:

$$(\Delta_{r,\phi} + k_{rn}^2) \cdot E_z(r,\phi) = 0 \qquad \textbf{(2.4.7)}$$

To solve the differential equation (2.4.7) we use again for $E_z(r,\phi)$ a statement of the type

$$E_z(r)\, E_z(\phi)$$

Since the fibre shows a rotational symmetry with respect to ϕ a useful solution in the sense of physics can only be obtained if we request $E_z(\phi) = E_z(\phi + 2\pi)$. This leads us to the following statement:

$$E_z(\phi) = e^{i \cdot p \cdot 2 \cdot \pi \cdot \phi},$$

with p as an integer. By substitution into equation (2.4.7) we get:

$$\Delta_{r,\phi}(E_z(r) \cdot E_z(\phi)) + k_{rn}^2 \cdot E_z(r) \cdot E_z(\phi) = 0$$

$$\Delta_{r,\phi}(E_z(r) \cdot E_z(\phi)) = E_z(\phi) \cdot \Delta_r E_z(r) - E_z(r) \cdot \frac{p^2}{r^2} \cdot E_z(\phi)$$

$$\text{and } E_z(\phi) \cdot \left[(\Delta_r - \frac{p^2}{r^2} + k_{rn}^2) \cdot E_z(r) \right] = 0$$

Since $E_z(\phi)$ is not always zero, the bracket must be zero. After multiplication with r^2

$$(r^2 \cdot \Delta_r - p^2 + r^2 \cdot k_{rn}^2) \cdot E_z(r) = 0$$

and evaluation of the Laplace operator which only acts on the radial components we finally get:

$$\left(r^2 \cdot \frac{\partial^2}{\partial r^2} + r \cdot \frac{\partial}{\partial r} + r^2 \cdot k_{rn}^2 - p^2 \right) \cdot E_z(r) = 0 .$$

Let's follow our habits and substitute $r\, k_m = x$ and $E_r = y$. The result will be:

$$x^2 \cdot \frac{\partial^2 y}{\partial x^2} + x \cdot \frac{\partial y}{\partial x} + (x^2 - p^2) \cdot y = 0 \qquad \textbf{(2.4.8)}$$

2.5 Solving the Wave Equation with Bessel Functions

This is the differential equation for cylindrical functions. Only for special values of p it can be represented by elementary functions. This differential equation kept Mr. Bessel (1784-1895), Mr. Neumann (1798-1895) and Mr. Hankel (1814-1899) restless till they found a solution. Anyhow, it was not found in connection with fibre optics. For the reader who worked on microwaves it is clearly visible that this equation is also used to solve problems of wave propagation within electric waveguides. The difference with respect to waveguides is that we consider non-conductive instead of conductive matter. A total of four solutions is known for equation (2.4.8). Generally these solutions are called cylindrical functions. Three basic types of cylindrical functions exist. The first type presumes integer values for p.

1. Type Bessel - Function $J_p(x)$, *p integer*

Neumann found the second type of cylindrical function. He presented the solution for non-integer values of p.

2. Type Neumann - Function $N_n(x)$, n arbitrary

Finally Hankel evaluated the third type of cylindrical function. He introduced a complex (Hankel function 1. type) and a complex conjugated (Hankel function 2. type) composition of Bessel- and Neumann-functions:

3. Type
$$H_p^{(1)} = J_p(x) + i \cdot N_p(x)$$
$$H_p^{(2)} = J_p(x) - i \cdot N_p(x)$$

For each of the presented solutions there exist also modified versions. Here *x* is substituted by *ix*. For the cladding of the fibre we need a solution which is real. Therefore the modified Hankel function is used here [4]. Since the differential equation (2.4.8) is homogenous (the right side = 0), also linear combinations of the solutions fulfil the equation. Fortunately the actual physical situation reduces the number of solutions. The Neumann- function has the property that it turns to infinity for x→0 or r → 0. That means that the fields would be infinite in the centre of the fibre. Since that is not in agreement with the reality this solution has to be disregarded. The Bessel-function has finite values in the centre of the fibre. For larger values of x or r the Neumann- and the Bessel-function oscillate like the sine or cosine. In so far the Bessel-function is a suitable solution for the core. For the cladding we need in addition an attenuation of the field. Here the modified Hankel-function offers a promising solution. For x→0 or r → 0 it turns to infinity but we only need it for the range r ≥ a (cladding). For the range r ≤ a (core) we shall use the Bessel-function. For solving the problems at the boundary between core and cladding we shall use the continuity conditions of the components of E and H for the transition from core to cladding and fit the Bessel- and Hankel-function for r = a. Let's find first the solution for the core. For any integer value of p the Bessel-function is:

$$J_p = \sum_{m=0}^{i=\infty} \frac{(-1)^m}{\prod(m) \cdot \prod(p+m)} \cdot \left(\frac{x}{2}\right)^{p+2m} \qquad \textbf{(2.5.1)}$$

$$\prod(m) = 1 \cdot 2 \cdot 3 \cdot \ldots\ldots \cdot m, \quad \prod(0) = 1$$

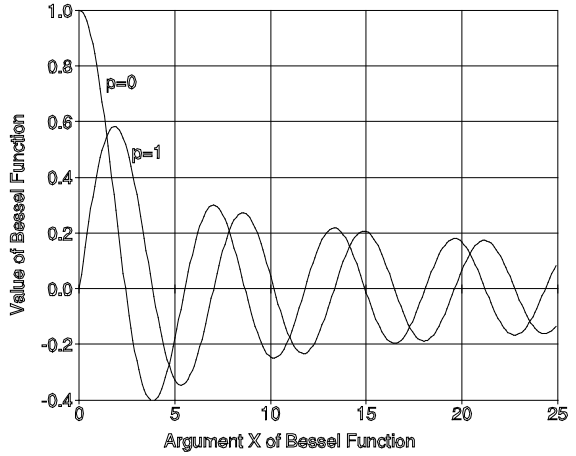

Fig. 5 : Bessel-function for p=0 and p=1

The solution of (2.4.7) is:

$$E_z(r,\phi)_k = C_E \cdot J_p(r \cdot k_{rn}) \cdot e^{i \cdot p \cdot 2 \cdot \pi \cdot \phi} \qquad \textbf{(2.5.2)}$$

$$H_z(r,\phi)_k = C_H \cdot J_p(r \cdot k_{rn}) \cdot e^{-i \cdot p \cdot 2 \cdot \pi \cdot \phi} \qquad \textbf{(2.5.3)}$$

with the range:

r ≤ a and $k_{rn}^2 = k_{rk}^2 = k^2 n_k^2 - \beta^2$.

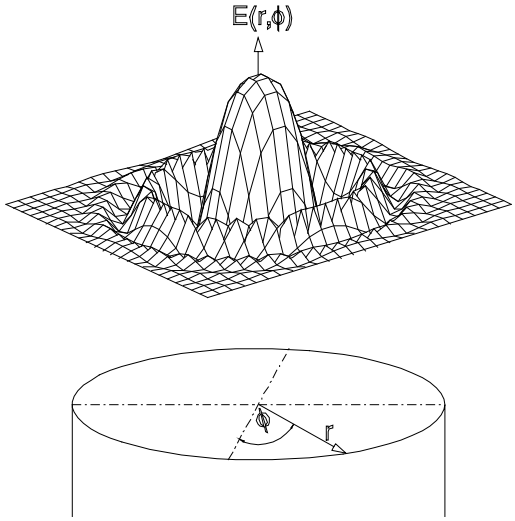

Fig. 6: Solution of Bessel-function for p=0

Fig. 6 presents the solution for *p=0.* Because of the ϕ dependence the rotational symmetry is lifted for solutions with p≠0. Already now we see how the electric field will establish within the core. It also gets clear that the radius a of the fibre will be decisive for the order *p* of the modes. In the radial direction of the fibre we observe a main maximum at *r = 0* and further aside maxima or minima which are also called nodes. The number of nodes, which will later be characterised by the counter index *q*, is determined by the diameter of the fibre as well as by the solution of the wave equation within the cladding. After having chosen a suitable cylindrical function for the solution within the cladding, it has to be ensured that it matches the continuity conditions for the electric and magnetic field at the boundary between core and cladding. This leads to the complete solution. For the waves within the cladding, r ≥ a , we want to achieve that the radial field of the core rapidly decreases in the cladding to favour the guidance of waves within the core. As solutions of the differential equation we use the modified Hankel-function: but which type? We first consider both types. The modified Hankel-function will be designated by *K:*

$$K_p^{(1)}(irk_{rm}) \approx \sqrt{\frac{2}{\pi \cdot r \cdot k_{rm}}} \cdot e^{irk_{rm}} \quad , rk_{rm} >> 1$$

$$K_p^{(2)}(irk_{rm}) \approx \sqrt{\frac{2}{\pi \cdot r \cdot k_{rm}}} \cdot e^{-irk_{rm}} \quad , rk_{rm} >> 1$$

(The detailed expansion of the modified Hankel-function is shown in chapter 6.1). The physical situation which we are facing requires that the fields E and H are attenuated monotonously in the cladding and approach zero for r → ∞. This can only be achieved by the Hankel-function $K^{(1)}$ under the condition that *rk* is purely imaginary. In this case the exponent of the e-function becomes real and negative which is necessary for attenuation. Let's remember, *r* is always real but

$$k_{rm}^2 = k^2 n_m^2 - \beta^2 \qquad k_{rm} = \sqrt{k^2 n_m^2 - \beta^2} \ ,$$

and k_m is imaginary if

$$\beta^2 > k^2 n_m^2 \qquad \textbf{(2.5.4)}$$

Here we get the first hint for the required coefficient of propagation β. Obviously the coefficient of propagation of the core must be greater than the coefficient of propagation of the cladding, since we defined initially β as coefficient of propagation of the core. Since *k* is the wave number of the considered light wave in vacuum and presuming that the coefficient of propagation of the core is the product of the vacuum wave number *k* and the refractive index n_k we can conclude that the refractive index of the cladding must be smaller than the refractive index of the core. This is the first consequence which we can extract from the solutions. It is in agreement with equation (2.3.1). The solution for the cladding of the fibre is now:

$$E_z(r,\phi)_m = D_E \cdot K_p^{(1)}(ik_{rn}r) \cdot e^{i \cdot p \cdot 2 \cdot \pi \cdot \phi}$$
$$H_z(r,\phi)_m = D_H \cdot K_p^{(1)}(ik_{rn}r) \cdot e^{-i \cdot p \cdot 2 \cdot \pi \cdot \phi}$$

We have:

r ≥ a and $k_{rn}^2 = k_{rm}^2 = k^2 n_m - \beta^2$.

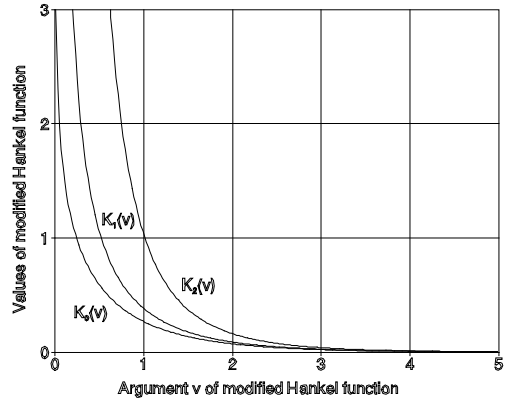

Fig. 7: Modified Hankel-function with v = $ik_{rm}r$

The constants $D_{E,H}$, $C_{E,H}$ and β have not yet been defined. These constants will be determined by the continuity conditions at the boundary for *r* = *a* . To perform these calculations we need the fields $E_r(r,\phi,z,t)$, $H_r(r,\phi,z,t)$, and $E_\phi(r,\phi,z,t)$, $H_\phi(r,\phi,z,t)$. We get them from the Maxwell equations.

$$\nabla \times \vec{H} = \varepsilon \cdot \varepsilon_0 \cdot \frac{\partial \vec{E}}{\partial t} \quad \text{and} \ \nabla \cdot \vec{H} = 0$$

$$\nabla \times \vec{E} = -\mu_0 \cdot \frac{\partial \vec{H}}{\partial t} \quad \text{and} \ \nabla \cdot \vec{E} = 0$$

Let's remember the rules for cylindrical coordinates:

$$\nabla \times \vec{\Psi}(r,\phi,z)\big|_r = \frac{1}{r} \cdot \frac{\partial \Psi_z}{\partial \phi} - \frac{\partial \Psi_\phi}{\partial z}$$

$$\nabla \times \vec{\Psi}(r,\phi,z)\big|_\phi = \frac{\partial \Psi_r}{\partial z} - \frac{\partial \Psi_z}{\partial r}$$

$$\nabla \times \vec{\Psi}(r,\phi,z)\big|_z = \frac{1}{r} \cdot \frac{\partial (r \cdot \Psi_\phi)}{\partial r} - \frac{1}{r} \cdot \frac{\partial \Psi_r}{\partial r}$$

and

$$\nabla \cdot \vec{\Psi} = \frac{1}{r} \cdot \frac{\partial (r \cdot \Psi_r)}{\partial r} + \frac{1}{r} \cdot \frac{\partial \Psi_\phi}{\partial \phi} + \frac{\partial \Psi_z}{\partial z},$$

So we will get the following four equations:

$$E_r = -\frac{i}{k_{rn}^2} \cdot \left[\beta \cdot \frac{\partial E_z}{\partial r} + \frac{\mu_o \cdot \omega}{r} \cdot \frac{\partial H_z}{\partial \phi} \right] \qquad \textbf{(2.5.5)}$$

$$E_\phi = -\frac{i}{k_{rn}^2} \cdot \left[\frac{\beta}{r} \cdot \frac{\partial E_z}{\partial \phi} - \mu_o \cdot \omega \cdot \frac{\partial H_z}{\partial r} \right] \qquad \textbf{(2.5.6)}$$

$$H_r = \frac{i}{k_{rn}^2} \cdot \left[\frac{\omega \cdot \varepsilon_0 n^2}{r} \cdot \frac{\partial E_z}{\partial \phi} - \beta \cdot \frac{\partial H_z}{\partial r} \right] \qquad \textbf{(2.5.7)}$$

$$H_\phi = -\frac{i}{k_{rn}^2} \cdot \left[\omega \cdot \varepsilon_0 n^2 \cdot \frac{\partial E_z}{\partial r} + \frac{\beta}{r} \cdot \frac{\partial H_z}{\partial \phi} \right] \qquad \textbf{(2.5.8)}$$

Here we will introduce the terms which are common in fibre optics and which we will use permanently in the following calculations.

Transversal phase unit $$u = k_k \cdot a = a \cdot \sqrt{n_k^2 k^2 - \beta^2} \quad \textbf{(2.5.9)}$$

Transversal attenuation unit $$\mathrm{v} = i k_m \cdot a = a \cdot \sqrt{\beta^2 - n_m^2 k^2}\,, \quad \textbf{(2.5.10)}$$

Fibre or frequency parameter $$V = ka \cdot \sqrt{n_k^2 - n_m^2} = \sqrt{u^2 + \mathrm{v}^2} \quad \textbf{(2.5.11)}$$

Phase parameter $$B = \frac{\beta^2 - k^2 n_m^2}{k^2\left(n_k^2 - n_m^2\right)} = \frac{\mathrm{v}^2}{u^2 + \mathrm{v}^2} \quad \textbf{(2.5.12)}$$

The continuity condition leads us to four equations which contain the four constants $D_{E,H}$, $C_{E,H}$. Regarding the solution procedure all steps are well represented in chapter 6.1. To get solutions for the constants which are unequal from zero their coefficient determinant has to be zero. This leads to the following characteristic equations which are at the same time the characteristic equations for the fibre.

$$\frac{J_{p+1}(u)}{J_p(u)} = \frac{n_m^2 + n_k^2}{2n_k^2} u X_p + \left\{ \frac{p}{u} - u\sqrt{\left(\frac{n_k^2 - n_m^2}{2n_k^2} X_p\right)^2 + p^2\left(\frac{1}{u^4} + \frac{1}{\mathrm{v}^2}\right)\cdot\left(\frac{n_m^2}{n_k^2}\frac{1}{\mathrm{v}^4} + \frac{1}{u^2}\right)} \right\} \quad \textbf{EH-Waves} \quad \textbf{(2.5.13)}$$

$$\frac{J_{p-1}(u)}{J_p(u)} = -\frac{n_m^2 + n_k^2}{2n_k^2} u X_p + \left\{ \frac{p}{u} - u\sqrt{\left(\frac{n_k^2 - n_m^2}{2n_k^2} X_p\right)^2 + p^2\left(\frac{1}{u^4} + \frac{1}{\mathrm{v}^2}\right)\cdot\left(\frac{n_m^2}{n_k^2}\frac{1}{\mathrm{v}^4} + \frac{1}{u^2}\right)} \right\} \quad \textbf{HE-Waves} \quad \textbf{(2.5.14)}$$

Both the equations (2.5.13) and (2.5.14) represent the characteristic equations for the four constants C_E, C_H, D_E and D_H and assure that the continuity requirements at the boundary between core and cladding are fulfilled. Since the Bessel-functions can not be represented analytically in an easy way, a graphical method shown in Fig. 8 is used to find a solution. Each of the left sides of the equations (2.5.13) and (2.5.14) is represented as a function of *u* for *p=2* . The left side of equation (2.5.14) has to be positive since it is required by the right side (since $X_p<0$).

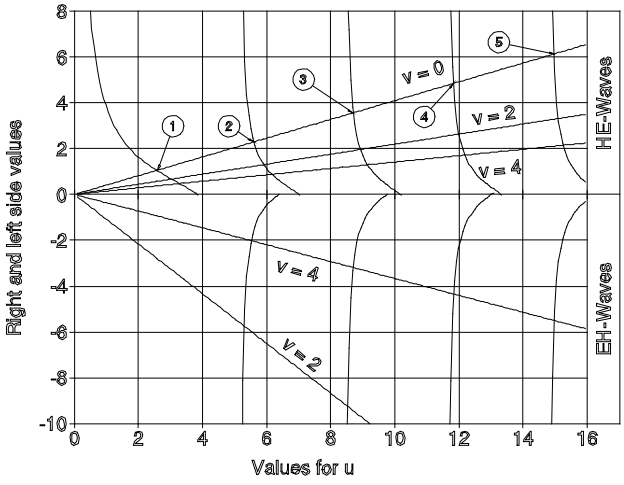

Fig. 8: Graphical solution of the characteristic equation for p=2

Therefore only positive values of $J(u)_{p-1}/J_p(u)$ have been represented. For equation (2.5.13) the negative values of $J(u)_{p+1}/J(u)_p$ are used correspondingly. The right side of the characteristic equation contains next to u the parameter

$$\mathrm{v} = a \cdot \sqrt{\beta^2 - n_m^2 k^2}$$

and the function $X_p = \dfrac{K_p'(\mathrm{v})}{\mathrm{v} \cdot K_p(\mathrm{v})}$, depending on v built up by the Hankel-function (see appendix 6.1). The points of intersection of the right side and left side curves of the characteristic equations provide the solutions which we are looking for. The solution area for positive values is denoted as the range of HE-waves the one for negative values as the range of EH-waves. This denomination has its historical roots in waveguide technology. Since the Bessel-functions are periodical there are several points of solution. All points of intersection of an area are numbered continually.

Fig. 9: The function $X_p(\mathrm{v})$ for *p=1* and *p=2*

The solutions of the right side for v = *0* play a particular role. In this case the limiting angle of total reflection is reached and the wave propagates even in the cladding without attenuation. Whenever a fibre is to guide the light within the core we have to have v>0. Let's remember that $u = a \cdot \sqrt{n_k^2 k^2 - \beta^2}$ and point out that increasing values of u signify an increasing fibre diameter a or an increase in the root value. In both cases this leads to an increasing number of nodes in the radial direction. Let's characterise the radial order defined by the point of

intersection of the left side of the characteristic equation with the right side by the number q. In consequence we can mark the types of waves of the corresponding solutions by *HEpq* or *EHpq*. A state characterised by a couple of values *p* and *q* is called a mode of the fibre. For each point of intersection there is one value for the fibre or frequency parameter *V*:

$$V_{pq}^{EH} = \sqrt{u_{pq}^2 + \mathrm{v}^2}$$

$$V_{pq}^{HE} = \sqrt{u_{pq}^2 + \mathrm{v}^2}$$

In Fig. 8, for example, 5 points of intersection at the limiting values for v=0 and p=2 are indicated. According to the notation rules they are called:

$$V_{21}^{HE}, V_{22}^{HE}, V_{23}^{HE}, V_{24}^{HE}, V_{25}^{HE}$$

The HE_{11} - wave plays a particular role. To recognise this the graphical solution of the characteristic equation is performed once again but this time for *p=1* (Fig. 10). The limiting curve for v→0 shows, that it tends to ∞ for v=0. So the point of intersection for *q=1* is at:

$$V_{11}^{HE} = \sqrt{u_{11}^{HE}} = 0$$

This means that each fibre will transmit this wave even if the core is extremely thin and the difference in refractive index extremely small. Because of the small attenuation value the wave will also propagate within the cladding. Therefore the HE_{11} - wave is the fundamental wave of the fibre. It has the smallest limiting value V of all waves.

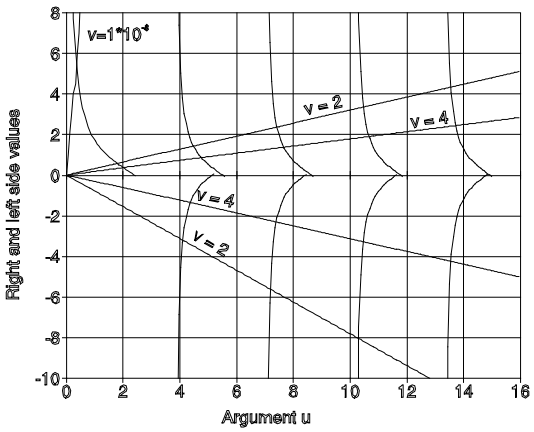

Fig. 10: Graphical solution of the characteristic equation for *p=1*

The limiting value of the characteristic equation for *p=0* is obtained from (2.5.14).

$$\frac{J_{-1}(u)}{J_0(u)} = \frac{-J_1(u)}{J_0(u)} = -u \cdot X_0(\mathrm{v})$$

Since $X_0(v=0)=\infty$, it must be $J_0(u)=0$. The first zero-transition of the Bessel-function for *p=0* is 2.405. So we get:

$$V_{01}^{HE} = u_{01} = 2.405$$

If a fibre with this parameter is used next to the fundamental wave HE_{11} also the HE_{01} wave is transmitted. But the latter one also propagates within the cladding. From Fig. 8 we see that the first limiting value of the HE_{21} wave is at

$$V_{21}^{EF} = u_{20} = 2.58$$

In so far it is only slightly above the HE_{01} wave. The HE_{0q} and EH_{0q} waves are symmetrical with respect to the radial direction or the axis because of *p=0* , that means they do not depend on the angle ϕ. Contrary to all other waves they are no hybrid waves with electric, E_z , and magnetic, H_z , field components in the direction of propagation.

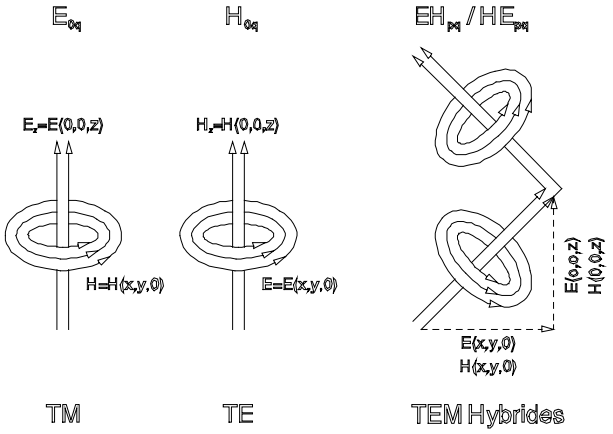

Fig. 11: Classification of field orientation

They are either purely „electric“ or purely „magnetic“ in the direction of propagation. A wave whose electric field strength points only into the z-direction has a magnetic field in the transversal direction. Instead of using EH_{0q} these waves are designated by E_{0q}. Since the magnetic field is transversal with respect to the direction of propagation we also speak about TM-waves (Transversal Magnetic waves). There are also waves which only have a magnetic field with respect to the direction of propagation. In consequence they have a transversal electric field. This all may be a bit confusing but is in agreement with the basic experience of current conducting wires which possess a transversal magnetic field. This, too, is reflected by Maxwell's equations:

$$\nabla \times \vec{H} = \varepsilon \cdot \varepsilon_0 \cdot \frac{\partial \vec{E}}{\partial t}$$

$$\nabla \times \vec{E} = -\mu_0 \cdot \frac{\partial \vec{H}}{\partial t}$$

In so far it is not a particular property of light conducting fibres but the consequence of the basic laws of nature. The Fig. 11 may contribute to further illustrations of hybrid waves particularly.

The designation EH (HE) is supposed to indicate that the amplitude of the E(H)-field is larger than the amplitude of the H(E) field in the direction of z. This corresponds

to the definitions in electrical engineering. Still, in fibre optics we will observe deviations from this rule.
If the fibre is made in a way that only the fundamental wave (*p=1* and *q=1*) is guided within the core the fibre is called a *monomode* or *singlemode* fibre. In all other cases we speak about *multimode* fibre. Depending on the range of application of the fibre one uses one or the other type of fibre. Let's now derive the „design"-rule for a fibre from the solutions allowing us to define the conditions under which a fibre „accepts" an incoming wave at given wavelength and guides it as a monomode fibre. For v=0 we have the limiting case with no reflection at the cladding. This means:

$$\mathrm{v}=a\cdot\sqrt{\beta^2-n_m^2k^2}=0\Rightarrow\beta^2=n_m^2k^2 \qquad \textbf{(2.5.15)}$$

For very weak guidance of the core wave we must request

$$\beta^2>n_m^2k^2$$

The other limit for β is received by requesting v→∞. In this way we get the highest possible attenuation within the cladding.

$$B=\frac{\beta^2-k^2n_m^2}{k^2\left(n_k^2-n_m^2\right)}=\frac{\mathrm{v}^2}{u^2+\mathrm{v}^2}=1$$

$$\beta^2=k^2\left(n_k^2-n_m^2\right)+k^2n_m^2=k^2n_k^2$$

Then the range of values of β for weak and strong guidance will be defined as follows:

$$n_m^2k^2<\beta\le n_k^2k^2 \qquad \textbf{(2.5.16)}$$

If the fibre is supposed to guide only the fundamental wave (*p=1*) and the node in radial direction is exactly on the boundary between core and cladding (*q=1*) , V is not to pass 2.405 since otherwise the wave HE_{01} will be transmitted. The condition for the transmission of the fundamental wave exclusively is then:

$$0<V\le 2.405$$

$$0<\frac{2\pi}{\lambda}a\sqrt{n_k^2-n_m^2}\le 2.405 \qquad \textbf{(2.5.17)}$$

Equation (2.5.17) represents an important prescription for the design of the fibre. It fixes the radius a of the core for monomode wave guidance if the wavelength λ and the refractive index for cladding and core have been selected. If, for example, the problem would be to transmit the light of a Helium-Neon laser (wavelength 633 nm, refractive index of core 1.5, refractive index of cladding 1.4) we would get the following range for the radius a:

$$a<2.405\cdot\frac{633\cdot10^{-9}}{2\pi\sqrt{(1.5)^2-(1.4)^2}}=0.45\mu m$$

The result depends strongly on the difference of the refractive index. The smaller this difference the greater can be the radius a.

2.6 Weakly guiding Fibres

Still, because of technical reasons it is not possible to choose the refractive index of the core much larger than the refractive index of the cladding. Since core and cladding are in close contact glasses of similar temperature coefficient can only be used. The consequence of this is the small difference in refractive index. For ordinary fibres it is

$$\frac{n_k-n_m}{n_k}\approx 2\cdot10^{-3},$$

where the refractive index n_k of the core is equal to 1.465 . If we use these values for the above mentioned example we get:

$$0<a<2.405\cdot\frac{633\cdot10^{-9}}{2\pi\sqrt{(1.465)^2-(1.462)^2}}=2.6\mu m$$

The diameter of the fibre should be chosen smaller than 5.2 µm to get the desired monomode transmission. Reconsidering this example we see that the difference in refractive index is fairly small in reality. Therefore we can write $n_m\approx n_k$ in good approximation. We are going to show that these step fibres possess a weak guidance for the core waves and some additional advantageous properties which we are going to check. We will calculate the characteristic equations anticipating that $n_m\approx n_k$. This simplifies equation (2.5.13) for EH-waves and equation (2.5.14) for HE-waves as follows:

$$\frac{J_{p-1}(u)}{J_p(u)}=-u\cdot\left(X_p+\frac{p}{\mathrm{v}^2}\right) \quad \textbf{HE-waves} \quad \textbf{(2.6.1)}$$

$$\frac{J_{p+1}(u)}{J_p(u)}=u\cdot\left(X_p-\frac{p}{\mathrm{v}^2}\right) \quad \textbf{EH-waves} \quad \textbf{(2.6.2)}$$

Let's use the identity (see chapter 6.1)

$$X_p=-\frac{K_{p\mp1}}{\mathrm{v}K_p}\mp\frac{p}{\mathrm{v}^2}$$

so we get:

$$u\cdot\frac{J_p(u)}{J_{p-1}(u)}=\mathrm{v}\cdot\frac{K_p(\mathrm{v})}{K_{p-1}(\mathrm{v})} \quad \textbf{HE-waves} \quad \textbf{(2.6.3)}$$

$$u\cdot\frac{J_{p+2}(u)}{J_{p+1}(u)}=\mathrm{v}\cdot\frac{K_{p+2}(\mathrm{v})}{K_{p+1}(\mathrm{v})} \quad \textbf{EH-waves} \quad \textbf{(2.6.4)}$$

Comparing both equations we can state that they only differ by the index p. Equation (2.6.4) has an index larger by 2 than equation (2.6.3). This means that all EH-waves with an index p reduced by 2 will have the same form as the HE-waves of index p. Since these waves are the eigenvalues of the solutions of the characteristic equation with the same value they are called „degener-

ated“ following the linguistic habits of quantum mechanics. Therefore they are not distinguishable:

$$HE_{p,q} = EH_{p-2,q}$$

Each linear combination of both waves with the same p and q values results in an eigenwave of the fibre, since for perfect degeneration the individual waves are at the same place at any time. The degeneration is only perfect if $n_k = n_m$. In reality the difference is so small that we can presume a perfect degeneration for all practical applications. Therefore the combination of $HE_{p,q}+EH_{p-2,q}$ leads to an eigenmode which can be expressed as follows:

$$\mathbf{LP_{l,q} = HE_{p,q}+EH_{p-2,q}}$$

In that way by superposition of the $HE_{2,q}$ and the $E_{0,q}$ wave the $LP_{1,q}$ wave is generated. The original properties of the EH, HE modes are superimposing to create the properties of the LP modes. This is particularly true for the polarisation of the waves. Since the EH and HE modes are already linearly polarised the LP modes are polarised as well. This is the reason for the designation LP standing for *linearly polarised.* If we accept that all EH and HE modes which distinguish in the order number p by 2 are superimposing to form the same LP mode then each $LP_{l,q}$ for *l>0* appears in 4 variations.

$$\begin{array}{lcll} HE_{2,q} & + & H_{0q} & \Rightarrow \quad LP_{1,q} \\ H_{0,q} & + & HE_{2,q} & \Rightarrow \quad LP_{1,q} \\ H_{E2,q} & + & E_{0,q} & \Rightarrow \quad LP_{1,q} \\ H_{0,q} & + & EH_{2,q} & \Rightarrow \quad LP_{1,q} \end{array}$$

Each two of these variations are mutually perpendicularly polarised.

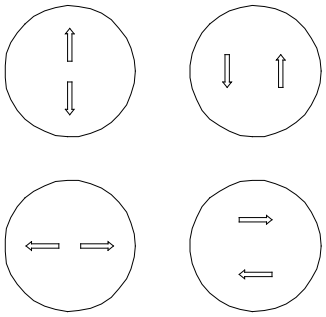

Fig. 12: The four variations of the LP_{11} mode. The arrows are pointing into the direction of the electric field strength which coincides with the direction of polarisation.

A particularity among the LP modes is the LP_{0q} mode. It ought to result out of a $HE_{1,q}$ and a $EH_{-1,q}$ mode. But this one does not exist so that the LP_{0q} mode only consists of the HE_{11} mode. Contrary to fibres with $n_k>n_m$ the transversal field part is dominant with respect to the longitudinal field part. That way the HE_{11} mode becomes independent of ϕ and rotation symmetrically within the weak conducting fibre. It is designated by LP_{01}. The LP_{01} wave is the fundamental wave of the weak conducting fibre and has two orthogonal directions of polarisation like all $HE_{1,q}$ or $LP_{0,q}$ waves. If we succeed in realising a less favourable coefficient of propagation for one direction, transmission in only one direction of polarisation will occur. This can be achieved by elliptical shaped fibres or anisotropic refractive index of the core. Meanwhile such fibres exist They are called „ polarisation preserving “. If linearly polarised light of a laser is coupled into such a fibre its direction of polarisation at the exit is the same as at the entrance. Fortunately we are now diving more and more into practice. Technically speaking the weak conducting fibre transmitting only the fundamental wave is the most important one. It is of special importance in communication technology because of the small transit time distortion. It is similar in laser technology where the coherence properties of the laser light have to be transmitted all along the fibre. Of importance are also multimode fibres for a large range of application in communication and control technology whenever the signals are to be transmitted at reduced speed and over distances which are not too large. Before the transit time distortions are discussed in detail we want to define the range which permits a weak conducting fibre just to guide the fundamental wave. For the LP_{01} wave the upper value of the fibre parameter is the same as for the HE_{11} wave since it is built up of it. Due to the numerical evaluation of the characteristic equation the lowest value is zero, but values <1.5 can not be taken into consideration since the transversal attenuation would become too small and the wave would hardly be guided within the core.

$$1.5 < V_{01}^{LP} \le 2.405$$

$$1.5 < \frac{2\pi}{\lambda} a\sqrt{n_k^2 - n_m^2} \le 2.405$$

This range differs only slightly from the fibre range of relatively high refractive index difference for the HE_{11} wave. But the LP_{01} or HE_{11} fundamental wave has the desired rotation symmetrical intensity distribution within the weak conducting fibre.

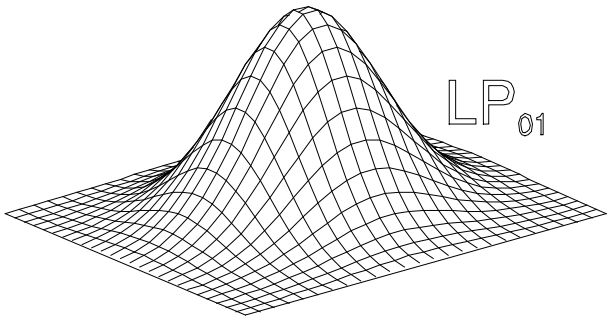

Fig. 13: Intensity distribution of the LP_{01} wave

2.7 Coupling of light

We are facing the problem to couple a beam of light to a fibre, respectively to introduce it into a fibre, the diameter of which is in the order of magnitude of 4-10 µm and in so far comparable to the wavelength of light. To get a sufficient high excitation of the fundamental mode of the

fibre, the beam of the light source has to be focused to a diameter of this order of magnitude. Under these circumstances the laws of geometrical optics fail because they anticipate parallel light beams or plane light waves which in reality exist only in approximation.

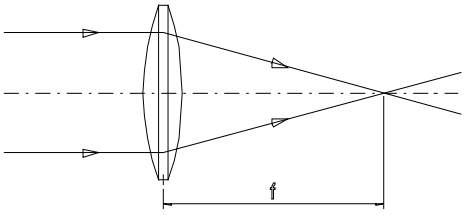

Fig. 14: Focusing two beams in geometrical optics

Real parallel light beams do not exist in reality and plane wave fronts exist only at a particular point. The reason for the failure of geometrical optics is the fact that it has been defined at a time where the wave character of light was still as unknown as the possibility to describe its behaviour by Maxwell's equations. To describe the propagation of light we use the wave equation

$$\Delta\vec{E} - \frac{n^2}{c^2}\cdot\frac{\partial^2\vec{E}}{\partial t^2} = 0$$

Solving this equation for the fibre we anticipated waves propagating within the fibre as a cylindrical body

$$\vec{E} = \vec{E}(r,\phi,z) \text{ with } r^2 = x^2 + y^2$$

Without boundary light would propagate as a spherical wave in all directions of the space.

$$\vec{E} = \vec{E}(r) \text{ with } r^2 = x^2 + y^2 + z^2$$

When we consider the technically most important case of spherical waves propagating in the direction of z within a small solid angle we arrive at the following statement for the electrical field:

$$\vec{E} = \vec{E}(r,z) \text{ with } r^2 = x^2 + y^2 + z^2$$

In this case the solution of the wave equation provides fields which have a Gaussian intensity distribution over the cross-section. Therefore they are called Gaussian beams. Similar to the solutions of the fibre the Gaussian beams exist in different modes depending on the actual boundary conditions. Such beams, especially the Gaussian fundamental mode (TEM_{00}) are generated with preference by lasers. But the light of any light source can be considered as the superposition of many such Gaussian modes. Still, the intensity of a particular mode is small with respect to the total intensity of the light source. The situation is different for the laser. Here the total light power can be concentrated in the fundamental mode. This is the most outstanding difference with respect to ordinary light sources next to the monochromasy of laser radiation. Gaussian beams behave differently from geometrical beams.

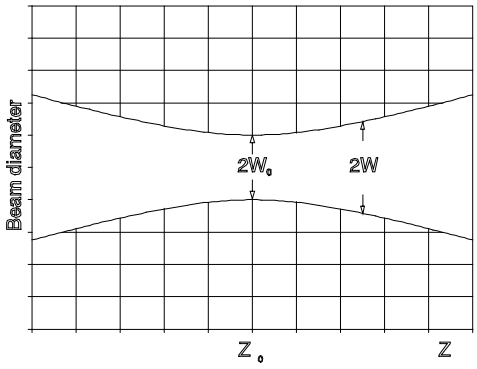

Fig.: 15: Beam diameter of a Gaussian beam as fundamental mode TEM_{00} and function of z.

A Gaussian beam always has a waist. The beam radius w results out of the wave equation as follows:

$$w(z) = w_0 \cdot \sqrt{1 + \left(\frac{z}{z_R}\right)^2}$$

w_0 is the smallest beam radius at the waist and z_r is the Rayleigh length

$$z_R = w_0^2 \frac{\pi}{\lambda}$$

In Fig.: 15 the course of the beam diameter as a function of z is represented. The beam propagates within the direction of z. At the position $z = z_0$ the beam has the smallest radius. The beam radius increases linearly with increasing distance. Since Gaussian beams are spherical waves we can attribute a radius of curvature of the wave field to each point z. The radius of curvature R can be calculated using the following relation:

$$R(z) = z + \frac{z_r^2}{z}$$

This context is reflected by Fig. 16. At $z = z_r$ the radius of curvature has a minimum . Then R increases with 1/z if z tends to $z = 0$. For $z=0$ the radius of curvature is infinite. Here the wave front is plane. Above the Rayleigh length z_r the radius of curvature increases linearly. This is a very essential statement. Due to this statement there exists a parallel beam only in one point of the light wave, to be precise only in its focus. Within the range

$$-z_r \le z \le z_r$$

a beam can be considered as parallel or collimated in good approximation. In Fig. 17 the Rayleigh range has been marked as well as the divergence Θ in the distant field, that means for $z>>z_0$. The graphical representations do not well inform about the extremely small divergence of laser beams another outstanding property of lasers.

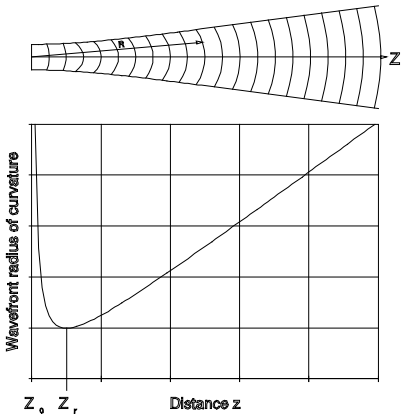

Fig. 16: Course of the radius of curvature of the wave front as a function of the distance from the waist at z=0

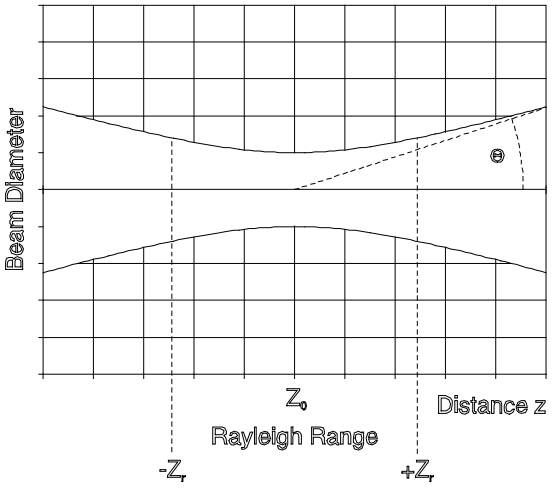

Fig. 17: Rayleigh range z_R and divergence Θ for the far field $z>>z_R$

The reason for this is that the ration of the beam diameter with respect to z has not been normalised. Let's consider, for example, a HeNe-Laser (632 nm) with a beam radius of $w_o=1mm$ at the exit of the laser. For the Rayleigh range 2 z_r we get:

$$2 \cdot z_R = 2w_0^2 \frac{\pi}{\lambda} = 2 \cdot 10^{-6} \frac{3.14}{623 \cdot 10^{-9}} = 9,9\ m$$

To get a maximum of power into the fibre a coupling optic of focal distance f is required assuring the coupling of a Gaussian beam into a weak guiding step index fibre in the LP_{01} fundamental mode.

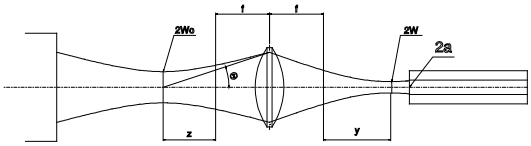

Fig. 18: For the calculation of the coupling optic

The radius at the waist is

$$w = \frac{w_0 \cdot f \cdot \theta \cdot}{\sqrt{w_0^2 + \theta^2 \cdot z^2}}$$

The position of the waist is:

$$y = \frac{z \cdot f^2}{z^2 + \left(\frac{w_0}{\theta}\right)^2}$$

Example: The beam of a HeNe laser of 0.5 mm diameter and of 1.5 mrad divergence is to focus by means of a lens. The focal distance is 50 mm and the lens is at a distance of 2 m from the laser. We find:

$$w = \frac{0,5 \cdot 10^{-3} \cdot 0,05 \cdot 1,5 \cdot 10^{-3}}{\sqrt{0,25 \cdot 10^{-6} + 2,25 \cdot 10^{-6} \cdot (2 - 0,05)^2}} = 12,6 \mu m$$

$$y = \frac{(2 - 0,05) \cdot 2,5 \cdot 10^{-6}}{(2 - 0,05)^2 + \left(\frac{0,5}{1,5}\right)^2} = 1,25 \mu m$$

For this example the position y of the waist coincides with the focus in good approximation and the radius of the waist is here 12.6 µm. To get the fibre under consideration adapted in an optimal way the focal distance f has to be chosen in a way that the radius of the beam is equal to the radius of the core. When laser diodes are used the preparation of the beam becomes more complicated.

2.8 Laser diodes

The laser diodes are a special class of lasers. They differ from „conventional" lasers in two points:

1. For the classical lasers the laser-active atoms (molecules or ions) are independent of one another and only the same energy levels are used for the laser process. This means in principle that in order to produce a population inversion an infinite number of atoms can contribute (Boltzmann statistics).

2. This is not the case with semiconductor lasers. Here a defined energy level can only be occupied by two active particles (electrons, Pauli principle). But in semiconductors, the wave functions of the individual atoms overlap to form a common energy band and the extent to which the level is occupied follows the Fermi Dirac statistics. When considering the laser process, the transition between the distribution of population in two energy bands instead of two energy levels must be taken into account as for conventional lasers.

Laser diodes do not have any inherently defined emission wavelength, because there are no two discrete energy levels that are responsible for the laser process as with traditional lasers, but rather an energy distribution

of electrons in energy bands. The second important difference concerns the propagation of the laser light within the pn zone. The spatial intensity distribution of the laser beam is defined by the laser medium and not by the resonator as for normal lasers. The goal of this experiment is also the understanding and checking of the basic facts. Therefore the difference between a laser with two discrete energy levels and the semiconductor laser with the typical band structure will be discussed in the following.

2.8.1 The energy band model

Atoms or molecules at large distance (compared to the spatial dimensions) to their neighbours do not notice mutually their existence. They can be considered as independent particles. Their energy levels are not influenced by the neighbouring particles.

The behaviour will be different when the atoms are approached as it is the case within a solid body. Depending on the type of atoms and their mutual interaction the energy states of the electrons can change in a way that they even can abandon „their" nucleus and move nearly freely within the atomic structure. They are not completely free, otherwise they could leave the atomic structure.

How the „free" electrons behave and how they are organised will be the subject of the following considerations. From the fundamentals of electrostatics we know that unequal charges attract. Therefore it is easy to imagine that an atomic structure is formed by electrostatic forces.

In the following we will call it „crystal". However, this model will fail latest when we try to justify the existence of solid Argon just by freezing it sufficiently. Since there is obviously some sort of binding within the crystal structure in spite of the fact that inert gases are neutral there must be additional forces which are responsible for this binding.

To understand these forces we must call on quantum mechanics for help. At the beginning this may be at bit difficult but it simplifies the later understanding. The Hamilton operator and Schroedinger's equation are supposed to be known. But the acceptance of the result of the following expertise on exchange interaction, exchange energy and tunnel effect for the formation of energy bands will be sufficient for further understanding provided quantum mechanics is considered as the background of all.

2.8.1.1 The binding of the hydrogen molecule

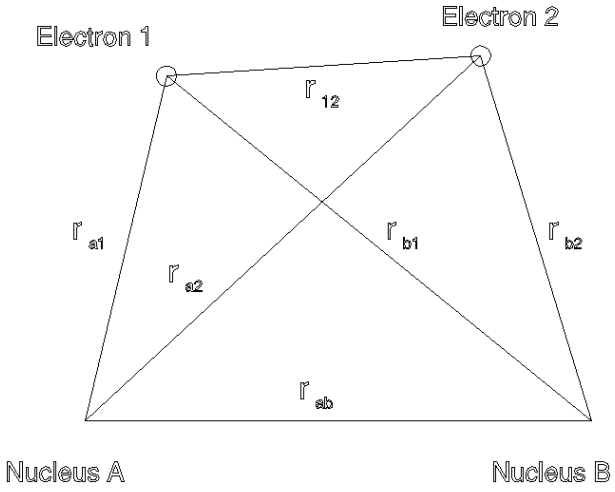

Fig. 19: Interaction of two hydrogen molecules

The total electric potential energy is:

$$U = -e^2 \cdot \left(\frac{1}{r_{a1}} + \frac{1}{r_{b2}} + \frac{1}{r_{b1}} + \frac{1}{r_{a2}} - \frac{1}{r_{ab}} \right) \quad \textbf{(2.8.1)}$$

The following Schroedinger equation has to be solved:

$$\Delta\Psi_1 + \Delta\Psi_2 + 8\pi^2 \frac{m}{h^2} \cdot (E - U) \cdot \Psi = 0$$

For two hydrogen atoms without interaction the total energy will be

$$E = E_0(1) + E_0(2) = 2E_0$$

Correspondingly the eigenfunction ψ is the product of the eigenfunctions of the individual electrons belonging to the nuclei a and b.

$$\Psi_{12} = \Psi_a(1) \cdot \Psi_b(2)$$

Since we can not distinguish between the individual electrons also the following linear combinations are valid eigenfunctions:

$$\Psi_{anti} = \Psi_a(1) \cdot \Psi_b(2) + \Psi_a(2) \cdot \Psi_b(1)$$
$$\Psi_{sym} = \Psi_a(1) \cdot \Psi_b(2) - \Psi_a(2) \cdot \Psi_b(1)$$

At the same time Pauli's principle has to be respected, that means the eigenfunction ψ_{ant} contains additionally the antiparallel spins (↑↓ + ↑↓) and the function ψ_{sym} the parallel spins (↑↑ - ↓↓). The electron distribution described by the linear combinations depends also on the distance dependent mutual electrostatic disturbance. As disturbance we have to consider the terms

$$\Delta U = -e^2 \cdot \left(\frac{1}{r_{b1}} + \frac{1}{r_{a2}} - \frac{1}{r_{ab}} \right)$$

which are the reason for the mutual interaction. To get the complete solution we have to add a „disturbance"-term to the undisturbed eigenfunctions ψ_a and ψ_s , as well as to the undisturbed energy. Then Schroedinger's

equation will no more be homogenous but inhomogeneous because of the additional „disturbance"-term. As solution (see **[5]**) we get:

$$E_{sym} = 2E_0 + e^2 \cdot C + e^2 \cdot A$$
$$E_{anti} = 2E_0 + e^2 \cdot C - e^2 \cdot A$$

We see that a term with the constant C representing the Coulomb part and a term with the constant A representing the interaction are added to the undisturbed energy. The exchange energy is based on the fact that electron 1 is localised near to nucleus A at a particular instant and near to nucleus B at another instant. The sign of A can be positive or negative. The energy difference between the two possible energies is just

$$\Delta E = E_{sym} - E_{anti} = 2 \cdot e^2 \cdot A$$

A detailed calculation **[5]** results in the following relation for C:

$$C = \int \left(\frac{1}{r_{ab}} - \frac{1}{r_{a2}} - \frac{1}{r_{b1}} + \frac{1}{r_{12}} \right) \cdot \Psi_a^2(1) \cdot \Psi_b^2(2) d^3r$$

and for A:

$$A = \int \left(\frac{1}{r_{ab}} - \frac{1}{r_{a2}} - \frac{1}{r_{b1}} + \frac{1}{r_{12}} \right) \Psi_a(1) \Psi_b(2) \Psi_a(2) \Psi_b(1) d^3r$$

Under respect of the fact that $\psi_a^2(1)$ and $\psi_b^2(2)$, integrated over the whole space represent probability densities which, multiplied by the elementary charge e, provide the total charge density ρ of the electrons 1 or 2 near the nuclei A or B, the constant C can also be written as:

$$e^2 C = \frac{e^2}{r_{ab}} - \int \frac{e^2 \rho_1}{r_{b1}} d^3r_1 - \int \frac{e^2 \rho_2}{r_{b2}} d^3r_2 + \iint \frac{e^2 \rho_1 \rho_2}{r_{12}} d^3r_1 d^3r_2$$

We see that C results out of the attracting or repulsing Coulomb forces. The exchange integral A looks very much like the Coulomb integral. But the electron densities $\psi^2_a(1)$ resp. $\psi^2_b(2)$ have been replaced by the mixed terms $\psi_a(1)\,\psi_b(2)$ and $\psi_a(2)\,\psi b(1)$ which are the result of the electron exchange. Here we can summarise as follows: If atoms are mutually approached the states of the undisturbed energy levels split into energetically different states. The number of newly created energy states are corresponding to the number of exchangeable electrons. (Fig. 20).

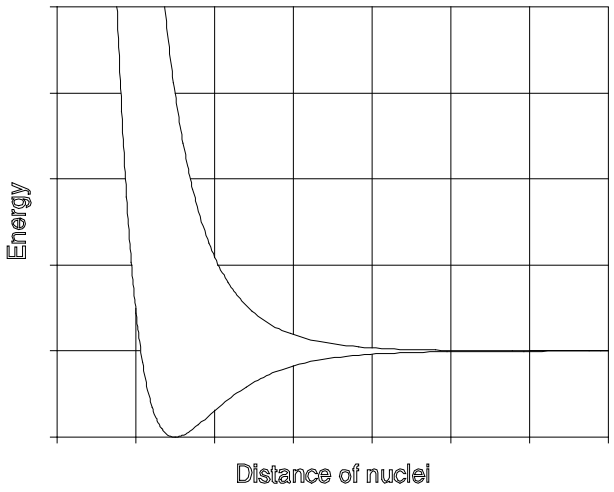

Fig. 20: Potential energy due to interaction of two hydrogen atoms

One of the curves shows a minimum for a particular distance of the atoms. No doubt, without being forced the atoms will approach till they have acquired the minimum of potential energy. This is also the reason for hydrogen to occur always as molecular hydrogen H_2 under normal conditions. The second curve does not have such a distinct property. The curves distinguish in so far as for the binding case the spins of the electrons are anti parallel. For the non-binding case they are parallel. It is easy to imagine that an increase of the number of atoms also increases the number of exchangeable electrons and in consequence also the number of newly generated energy levels. Finally the number of energy levels is so high and so dense that we can speak about an energy band.
Here it is interesting to compare the action of the electrons with the behaviour of ambassadors.

The electrons in the most outside shell will learn first about the approach of an unknown atom. The eigenfunctions will overlap in a senseful way. One electron will leave the nucleus temptatively to enter an orbit of the approaching atom. It may execute a few rotations and then return to its original nucleus.

If everything is O.K. and the spins of the other electrons have adapted appropriate orientations new visits are performed. Due to the visits of these „curious" electrons the nuclei can continue their approach. This procedure goes on till the nuclei have reached their minimum of acceptable distance. Meanwhile it can no more be distinguished which electron was part of which nucleus.

If there is a great number of nuclei which have approached in this way there will also be a great number of electrons which are weakly bound to the nuclei. Still, there is one iron-rule for the electrons: my energy level can only be shared by one electron with opposite spin (Pauli principle). Serious physicists may now warn to assume that there may be eventually male and female electrons. But who knows.....

Let's return to incorruptible physics.

Up to now we presumed that the atom only has one electron. With regard to the semiconductors to be discussed later this will not be the case. Discussing the properties of solid bodies it is sufficient to consider the valence electrons that means the most outside located electrons only as it has been done for separated atoms. The inner electrons bound closely to the nucleus participate with a rather small probability in the exchange processes. Analogously to the valence electrons of the atoms there is the valence band in solid bodies. Its population by electrons defines essentially the properties of the solid body. If the valence band is not completely occupied it will be responsible for the conductivity of electrons. A valence band not completely occupied is called

conduction band.

If it is completely occupied the next not completely occupied band will be called conduction band.

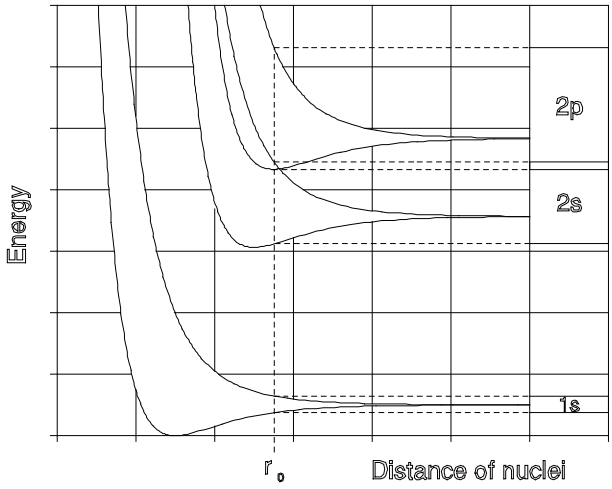

Fig. 21: Band formation by several electrons. The most outside electrons are responsible for the equilibrium distance r_0.

In the following section the question is to be answered how the density of states of a band of electrons looks like and on which quantities it depends. Before doing that and for reasons of completeness another attempt is made to determine the electron distribution within a solid body.

2.8.1.2 Periodic potentials

Although quantum mechanics is fairly powerful, up to now one has not succeeded to calculate the energy eigenvalues of complex atoms and molecules. One generally relies on skilful statements for the energy potentials to which the electrons are submitted. The statement of periodical potentials has been found to be especially powerful. A clear presentation is found in **[5]** and **[8]**. We follow the outlining by statistical considerations.

2.8.1.3 Fermi distribution

In Fig. 21 we have shown that the energy bands are the result of the mutual interaction of the atoms. Each band has a particular width ΔE, the magnitude of which is determined by the exchange energy and not by the number N of the interacting atoms. Furthermore we know that the number of energy levels within a band is determined by the number of interacting electrons. The Pauli principle states that such a level can only be occupied by two electrons. In this case the spins of the electrons are antiparallel. Within a band the electrons are free to move and they have a kinetic energy of

$$E = \frac{1}{2} m \mathrm{v}^2 \text{ or } E = \frac{p^2}{2m}$$

The mass of the electron is m, v the velocity and p the impulse. The constant potential energy will not be taken into consideration. Furthermore we will set the energy of the lower band edge to zero. The maximum energy E_{max} of an electron within a band can not pass the value ΔE since otherwise the electron would leave the band and no longer be a part of it. Consequently we can write:

$$E_{\max} = \Delta E = \frac{1}{2m} p_{\max}^2 .$$

We still have to find out how many electrons of energy E $\leq E_{max}$ exist and within a second step we wish to know how many electrons exist in the energy interval dE. To reach this goal we will use a trick already applied in deriving the number of modes in a cavity resonator.(see EXP01 Emission & Absorption). But here we will consider electrons instead of photons. The course of considerations will be the same since we can attribute to each electron a wave with wave vector k. For the impulse p we write:

$$\vec{p} = \hbar \cdot \vec{k}$$

Only such electron energies are permitted within a volume the wave functions of which are zero at the walls. To express it in a more simple way: an integer multiple of half the wavelength λ of the associated standing wave must fit, for instance, into the length L of a cube:

$$L_x = n_x \frac{\lambda}{2} \text{ and } k_x = \frac{2\pi}{\lambda}$$

For the electron energy of the cube we get:

$$E = \frac{p^2}{2m} = \frac{\hbar^2}{2m} \vec{k} \cdot \vec{k} = \frac{\hbar^2}{2m} \left(k_x^2 + k_y^2 + k_z^2 \right)$$

$$E = \frac{2h^2}{m} \left(\frac{n_x^2}{L_x^2} + \frac{n_y^2}{L_y^2} + \frac{n_z^2}{L_z^2} \right) = \frac{2h^2}{mL^2} \left(n_x^2 + n_y^2 + n_z^2 \right)$$

Let's remember the equation of a sphere

$$R^2 = x^2 + y^2 + z^2$$

and compare it with the equation for E. We recognise an analogous equation of the following type:

$$E\frac{mL^2}{2h^2} = \left(n_x^2 + n_y^2 + n_z^2\right)$$

or with $E = \frac{\hbar^2 k^2}{2m}$:

$$L^2\frac{k^2}{\pi^2} = n_x^2 + n_y^2 + n_z^2$$

The radius of this sphere is Lk/π and n_1, n_2, n_3 are the x y z coordinates. As n is an integer and positive they only generate one eighth of a complete sphere set up by a spatial lattice with lattice constant 1. Permissible are only such wave vectors $\vec{k}$, the components of which are coinciding with the n values or, to express it differently, each point of intersection of the lattice represents a valid solution for the wave vector k of a stationary wave. The answer to the initially raised question regarding the number of electrons for a particular length L of a potential box results now out of the counting of the number of points of intersection. Fig. 22.

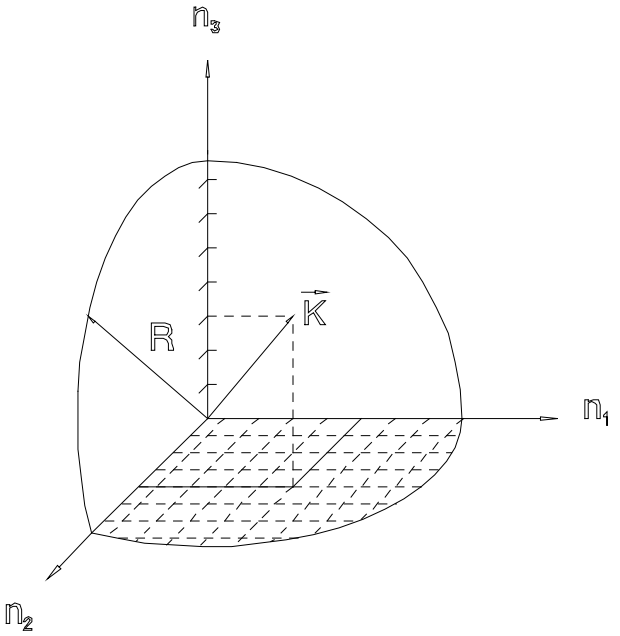

Fig. 22: Calculation of the electron density

This work can also be done analytically. If one uses the formula for the volume of a sphere $V_{sphere} = 4/3\ \pi\ R^3$ one gets for one eighth of a sphere with a radius for an upper limit of energy at E_{max}:

$$N\left(E_{\max}\right) = \frac{1}{8}\cdot\frac{4}{3}\pi\cdot\left(L\frac{k}{\pi}\right)^3$$

with $E = \frac{\hbar^2 k^2}{2m}$ or $k^2 = \frac{4\pi^2}{h^2}2mE$ one gets:

$$N\left(E\right) = \frac{8}{3}\frac{\pi}{h^3}V\cdot\left(2mE\right)^{3/2}$$

Here V is the volume of the box. An additional factor of 2 accounts for the fact that two electrons are admitted in each state if their spins are antiparallel. Let's divide *N(E)* by the volume V to get the electron density

$$n\left(E\right) = \frac{8}{3}\frac{\pi}{h^3}\cdot\left(2mE\right)^{3/2}$$

The electron density per unit energy dn(E)/dE is found by differentiation:

$$dn\left(E\right) = \frac{4\pi}{h^3}\left(2m\right)^{3/2}\sqrt{E}\cdot dE$$

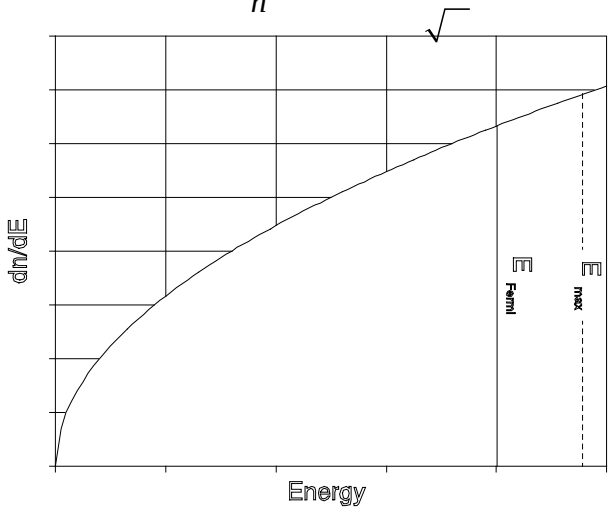

Fig.: 23: Number of electrons per unit volume V and energy interval dE as a function of the energy E.

The situation in Fig.: 23 shows that the band has not been completely filled up since the Fermi energy is smaller than the maximal possible energy. This means that this band is a conduction band. If the Fermi energy would be equal to the maximal energy we would have a valence band. A transfer of this knowledge to the energy level scheme of Fig. 21 and a selection of the 2s band would provide the picture of Fig. 24.

Up to this point we anticipated that the temperature of the solid body would be 0 K. For temperatures deviating from this temperature we still have to respect thermodynamic aspects namely additional energy because of heat introduced from outside.
Fermi and Dirac described this situation using statistical methods. **[7]**. The electrons were treated as particles of a gas: equal and indistinguishable. Furthermore it was presumed that the particles obey the exclusiveness principle which means that any two particles can not be in the same dynamic state and that the wave function of the whole system is anti-symmetrical.

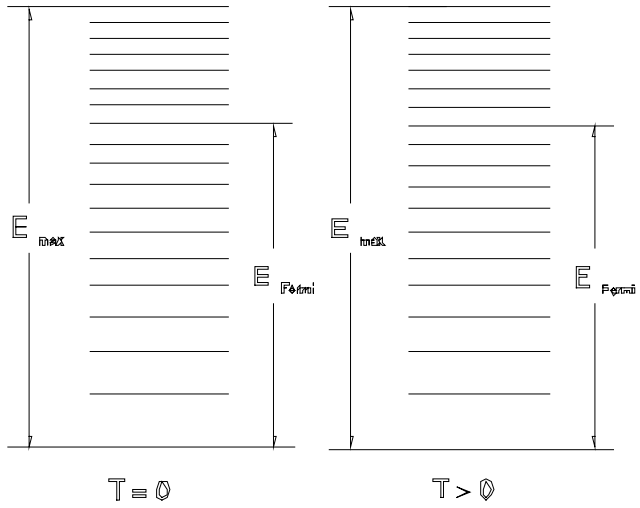

Fig. 24: Distribution of free electrons over the energy states within a conduction band

Particles which satisfy these requirements are also called Fermions. Correspondingly all particles which have a spin of 1/2 are Fermions and obey the Fermi Dirac statistics. Electrons are such particles. Under respect of these assumptions both physicists got the following equation for the particle density of the electrons within an energy interval dE:

$$\frac{dn(E)}{dE} = \frac{4\pi}{h^3}(2m)^{3/2} \cdot \frac{\sqrt{E}}{e^{\frac{E-E_{Fermi}}{kT}} + 1} \cdot dE$$

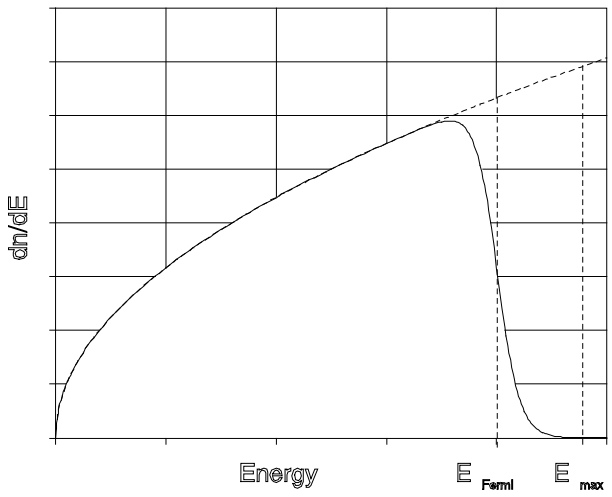

Fig. 25: Number of electrons per unit volume and energy interval dE as a function of the energy E, but for a temperature T > 0.

The above equation is illustrated by Fig. 25. As shown in Fig. 24 by introduction of thermal energy the „highest“ electrons can populate the states which are above them. Based on these facts we are well equipped to understand the behaviour of solid bodies. We are going to concentrate now our special interest on the semiconductors which will be presented in the next chapter with the help of the previously performed considerations.

2.8.2 Semiconductors

Before starting the description of the semiconductor with regard to its behaviour as „lasing“ medium we still have to study the „holes“.

States of a band which are not occupied by electrons are called „holes“. Whenever an electron leaves its state it creates a hole. The electron destroys a hole whenever it occupies a new state. The whole process can be interpreted in that way that the hole and the electron exchange their position Fig. 26. Also the holes have their own dynamic behaviour and can be considered as particles like the electrons.

It is interesting to note that the holes do have the exact opposite properties of the electrons. Since the temporary course of the holes' migration is the same as for the electron they have also the same mass except that the mass of the hole has the opposite sign. Furthermore its charge is positive.

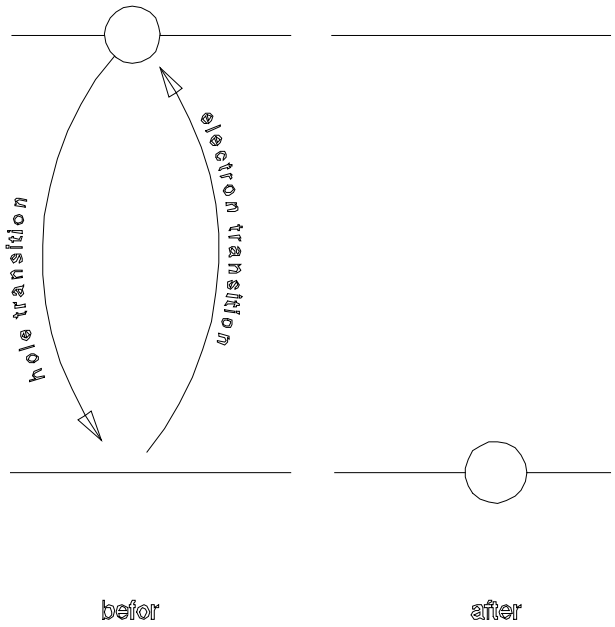

Fig. 26: Electron and hole transition

Once the existence of the holes has been accepted they also have to have a population density. It will be introduced in the following.

For this reason we complete Fig. 24, as shown in Fig. 27. It is easy to understand that on one side the holes are preferably at the upper band edge and on the other side their population density results out of the difference of the population density minus the population density of the electrons.

Fig. 28 shows the population density of the electrons. Fig. 29 shows the difference and in so far the population

density of the holes. Attention has to be paid to the fact that the abscissa represents the energy scale of the band and not the energy of the holes.

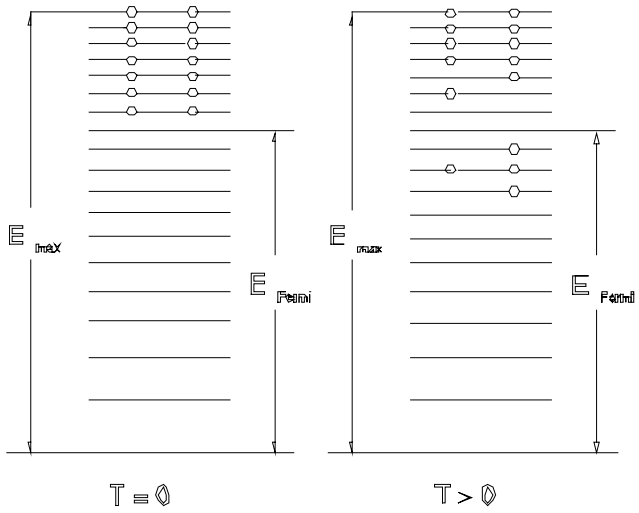

Fig. 27: Distribution of the holes and the electrons within an energy band

To prepare the discussion of optical transitions in semiconductors it gives a sense to modify the diagrams.

Until now the abscissa was used as energy scale for the diagrams of the state and population densities. For the presentation of optical transitions it is more practical to use the ordinate as energy scale.

To get use to it Fig. 28 has been represented in the modified way in Fig. 30. The shown population density refers to an energy scale for which the lower edge of the valence band has been set arbitrarily to zero.

The represented situation refers to a semiconductor where the distance between conduction and valence band is in the order of magnitude of thermal energy *(kT)*. Here the Fermi energy lies in the forbidden zone.

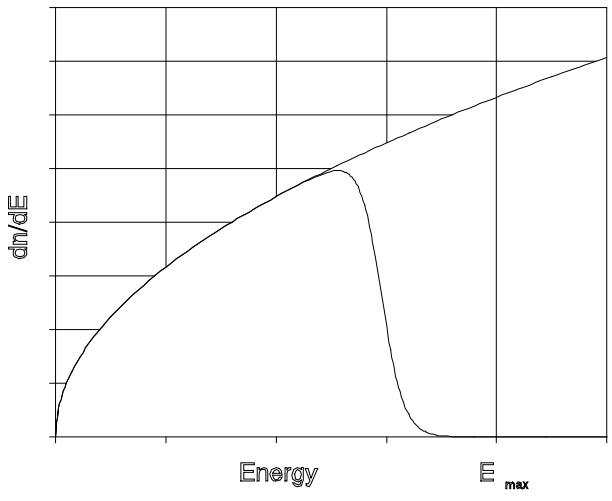

Fig. 28: Population density of the electrons

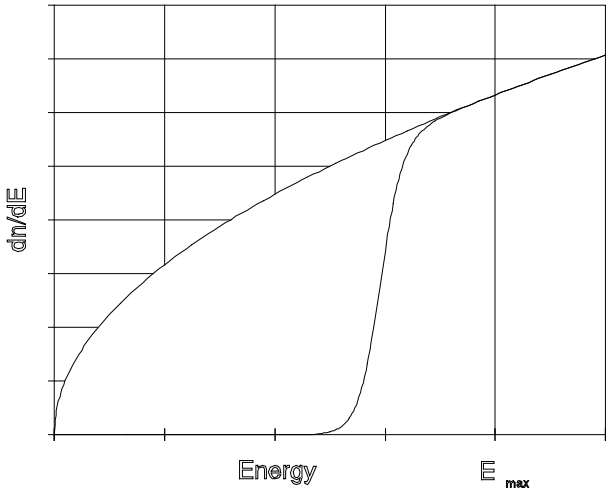

Fig. 29: Population density of the holes

Because of the thermal energy some electrons have left the valence band and created holes. For the following considerations it is sufficient to learn something about the population densities of the electrons in the conduction band as well as about the holes in the valence band. As will be shown later there are optical transitions from the conduction band to the valence band provided they are allowed. Near the lower band edge of the conduction band the state densities are admitted to be parabolic **[4]**. The same is true for the holes at the upper edge of the valence band. Fig. 31. The densities of states inform about the number of states which are disposed for population and the spectral distribution reflects how the electrons and holes are distributing over these states. Next to the band edges the spectral distribution fits to a Boltzmann distribution.

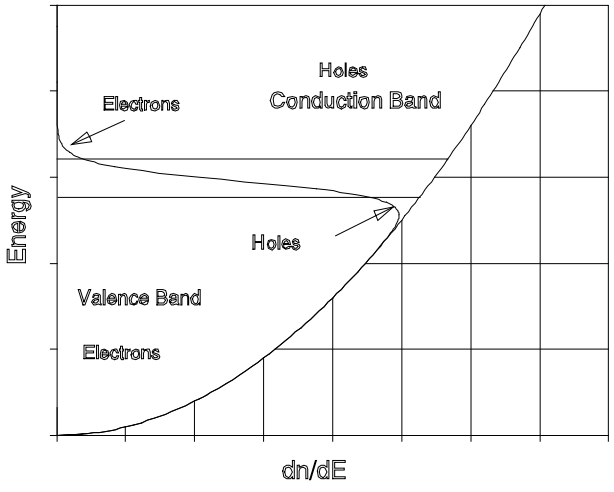

Fig. 30: Population density on the energy scale

If we succeed to populate the conduction band with electrons and to have a valence band which is not completely occupied by electrons (Fig. 14) electrons may pass from the conduction band to the valence band. That way a photon is generated. By absorption of a photon the inverse process is also possible.

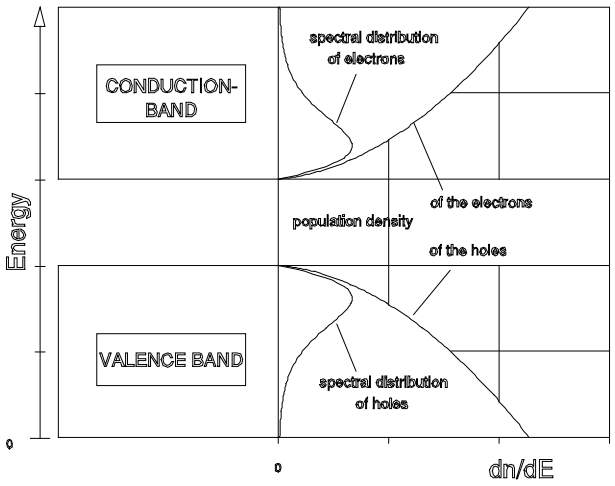

Fig. 31: Densities of states and spectral distributions

The following illustration Fig. 32 shows the situation of a population inversion in a semiconductor. Attention must be drawn to the fact that, until now, we only discussed a semiconductor consisting of one type of atoms. Consequently the situation shown in Fig. 32 is, at least for this type of direct semiconductor, only fictitious. It can only be created for very short intervals of time and can therefore not be taken into consideration for the realisation of a semiconductor laser. By doping the basic semiconductor material we can create band structures with different properties. A very simple example may be the semiconductor diode where the basic material, germanium or silicon, is converted into p or n conducting material using suitable donators and acceptors. By the connection of the doted materials a barrier (also called active zone) is formed. It will be responsible for the properties of the element.

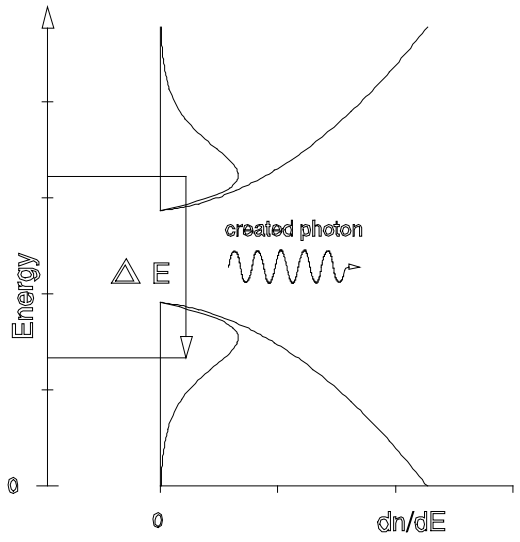

Fig. 32: Population inversion in a semiconductor for T > 0

Silicon is mainly used for highly integrated electronic circuits while ZnS is chosen as fluorescent semiconductor for TV screens. As light emitting diodes and laser diodes so called mixed semiconductors like AlGaAs are in use. Mixed semiconductors can be obtained whenever within the semiconductors of valence three or five individual atoms are replaced by others of the same group of the periodical system. The most important mixed semiconductor is aluminium gallium arsenide (AlGaAs), where a portion of the gallium atoms has been replaced by aluminium atoms. This type of semiconductor can only be produced by a fall out as thin crystal layer, the so called epitaxy layer, on host crystals. To perform this stress free it is important that the lattice structure of the host crystal (lattice matching) coincides fairly well with the lattices structure of AlGaAs. This is the case for GaAs substrate crystals of any concentration regarding the Al and Ga atoms within the epitaxy layer. In that way the combination of AlGaAs epitaxy layers and GaAs substrates offers an ideal possibility to influence the position of the band edges and the properties of the transitions by variation of the portions of Ga or Al.

2.8.3 Semiconductor laser

As simple as it may seem, it took about 20 years until people had acquired the necessary technology of coating under extremely pure conditions.
It all began in 1962 with the first laser diode, just two years after Maiman had demonstrated the first functional ruby laser. In the course of 1962 three different groups reported more or less simultaneously the realisation of GaAs diode lasers.

1.	R. N. Hall	General Electric
2.	M. I. Nathan	IBM
3.	T. M. Quist	MIT

The first laser was basically made of highly doted GaAs Fig. 33. A threshold current of 100 kA/cm^2 was needed since the GaAs material of those days was not by far as good as it is today regarding the losses within the crystal. Because of thermal conditions the laser could only work at 70 ^{0}K and in the pulsed mode. In the course of the following years the threshold could be lowered to 60 kA/cm^2 by improving the crystals but only the use of a hetero-transition (Bell Labs. and RCA-Labs.) brought the „break-through“ in 1968. The threshold could be lowered to 8 kA/cm^2 and working in the pulse mode at room temperature was possible Fig. 34.

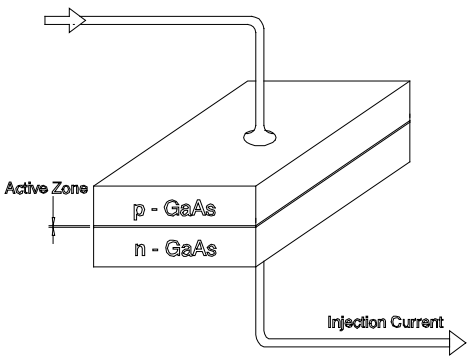

Fig. 33: Simple laser diode around 1962, working at

70 K and with 100 kA/cm^2 in the pulse mode.

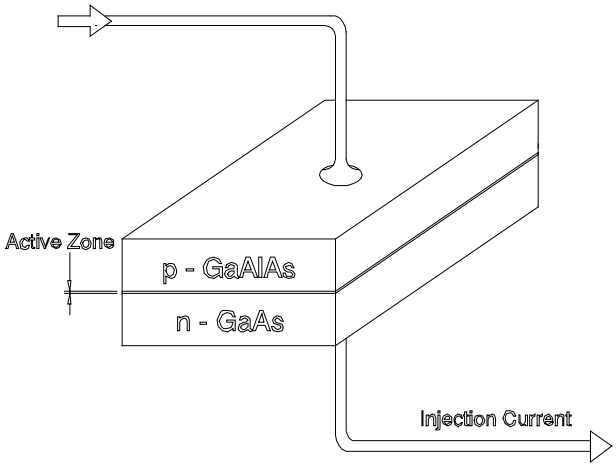

Fig. 34: Simple-hetero structured laser around 1968, working at 8 kA/cm^2 in pulse mode at room temperature.

In this concept a layer of p conducting GaAlAs is brought on the p layer of the pn transition of GaAs. The slightly higher band gap of GaAlAs compared to GaAs ensures that a potential barrier is created between both materials in a way that charge carriers accumulate here and the formation of inversion is increased respectively the laser threshold is remarkably lowered to 8 kA/cm^2 .
The next step in development was the attachment of a similar layer on the n-side of the crystal. That way the threshold could be lowered once again in 1970. Now it amounted to about 1 kA/cm^2. Until today nearly all commercially sold laser diodes are built up on the double hetero structure principle. (Fig. 36 and Fig. 37).

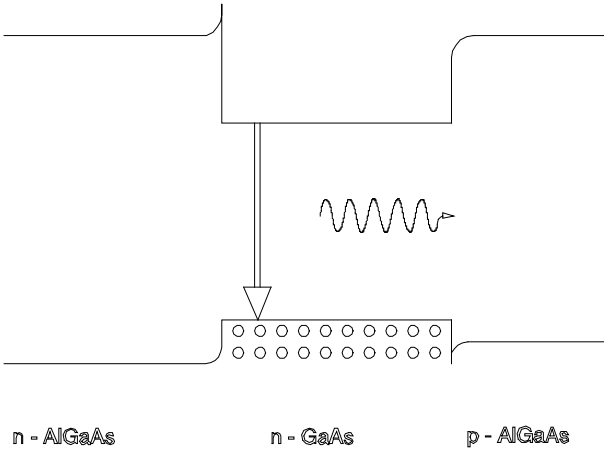

Fig. 35: Energy band diagram of a N n P - double hetero structure.

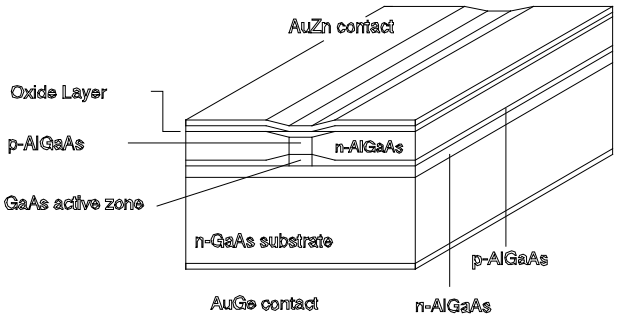

Fig. 36: „Buried“ hetero structure. The active zone has been buried between some layers which ensure an optimal beam guidance in the zone.

2.8.4 Resonator and beam guidance

As already mentioned at the beginning the diode laser differs from the „classical“ lasers in the dimensions of the resonator and in the propagation of the beam. For the diode lasers the active material represents the resonator at the same time. Furthermore the ratio of the resonator length (300 µm) to the wavelength (820 nm) is:

$$L / \lambda = 366 ,$$

For a HeNe-Laser (λ = 632 nm) with a typical resonator length of 20 cm this ratio is 3 $10^{8.}$ Considering additionally the lateral dimensions of the resonator we get a ratio of 12.5 for the diode lasers with a typical width of 10 µm for the active zone. With capillary diameters of the He-Ne tubes of about 1 mm one gets a value of 1582. This already indicates that the beam characteristics of the laser diode will distinguish significantly from „classical“ lasers.

2.8.5 Divergence and intensity distribution

Not only the beam guidance but also the size of the laser mirrors influences the beam geometry. Generally for conventional lasers the mirrors are very large compared with the beam diameter. The laser mirror (crystal gap area of the active zone) of the laser diodes has a size of about 10 µm x 2 µm, through which the laser beam has „to squeeze“ itself. Diffraction effects will be the consequence and lead to elliptical beam profiles. (Fig. 37).

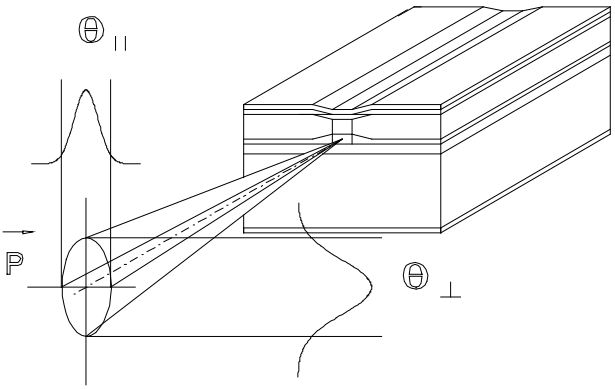

Fig. 37: Elliptical beam profile of a diffraction limited laser diode in the far field (some meters).

The polarisation is parallel to the "junction plane", that is the plane which is passed by the injection current perpendicularly. The divergence angles $\theta_{\perp}$ and $\theta_{||}$ differ by about 10-30° depending on the type of laser diode. If the beams are extended geometrically into the active medium the horizontal beams will have another apparent point of origin as the vertical beams. The difference between the points of origin is called astigmatic difference Fig. 38. It amounts to about 10 µm for the so called index guided diodes. For the so called gain guided diodes these values are appreciably higher. Modern diodes are mostly index guided diodes. This means that the laser beam is forced not to leave the resonator laterally by attaching lateral layers of higher refractive index to the active zone (Fig. 36). At the gain guided diodes the current is forced to pass along a small path (about 2-3 µm width).

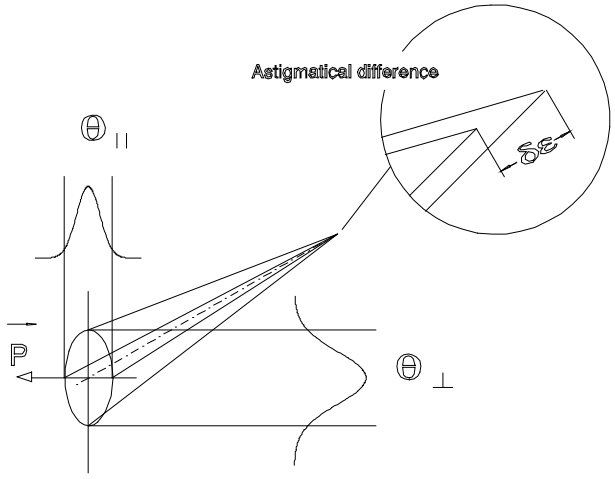

Fig. 38: Astigmatic difference δε

In this way the direction of the amplification (which is proportional to the current flux) and the laser radiation are determined. At the gain guided diodes the formation of curved wave fronts within the resonator is disadvantageous since they simulate spherical mirrors. In this case higher injection currents provoke transversal modes which will not appear in index guided diodes because of the plane wave fronts. Laser diodes with intensity profiles following a Gauss curve and a beam profile which is only limited by diffraction are called *diffraction limited lasers* (DFL). They represent the most „civilised“ diode lasers. For the time being they are only available for powers up to 200 mW. High power diode lasers as used, for example, to pump Nd YAG lasers partially have very fissured nearly rectangular intensity profiles.

2.8.6 Polarisation

It is understandable that the laser radiation of the diodes has a distinct direction of polarisation, since the height of the exit window is 4 times and the width 12.5 times larger than the wavelength. Because of the fraction of spontaneous emission the light of the laser diode also contains components oscillating in the vertical direction The ratio of polarisation, $P_{\perp}$ to $P_{||}$, depends on the output power since for higher laser power the ratio of spontaneous to stimulated emission is changing (Fig. 42).

2.8.7 Spectral properties

Another property of the diode laser is the dependence of its wavelength on the temperature (about 0.25 nm/°K) and on the injection current (about 0.05 nm/mA). Users who need a well defined wavelength have to adjust temperature and injection current in a way that the wavelength remains constant. By changing the temperature the wavelength of the laser radiation can be altered.

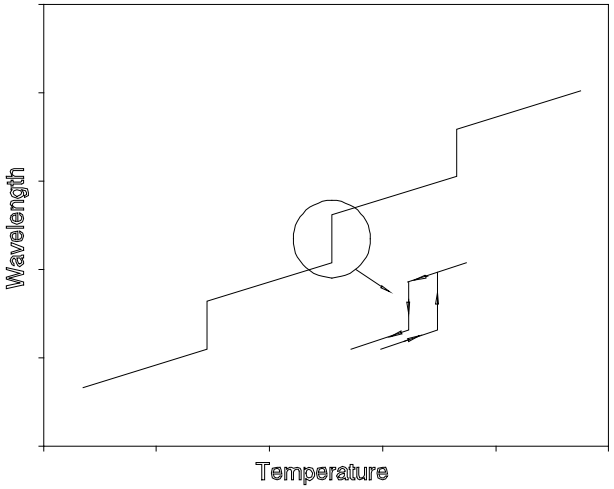

Fig. 39: Emission wavelength as a function of the crystal temperature of the laser diode and hysteresis.

The wavelength increases with increasing temperature. The reason for this is that the refractive index and the length of the active zone , respectively the resonator, increase with increasing temperature. Beyond a certain temperature the mode does not fit anymore into the resonator and another mode which faces more favourable conditions will start to oscillate.
As the distance between two successive modes is very large for the extremely short resonator (typical 300 µm), the jump is about 0.3 nanometer. Lowering the temperature gets the laser jumping back in his wavelength. After this the laser must not be necessarily in the departing mode. Applications anticipating the tuning ability of the laser diode should therefore be performed within a jump-free range of the characteristic line (Fig. 39).
A similar behaviour is observed for the variation of the injection current and in consequence for the laser output power. Here the change in wavelength is mainly the result of an increase in the refractive index which again is influenced by the higher charge density in the active zone. A higher output power provokes also a higher loss of heat and an increase in temperature of the active zone. The strong dependence of the current and the output power on the temperature are typical for a semiconductor (Fig. 40).

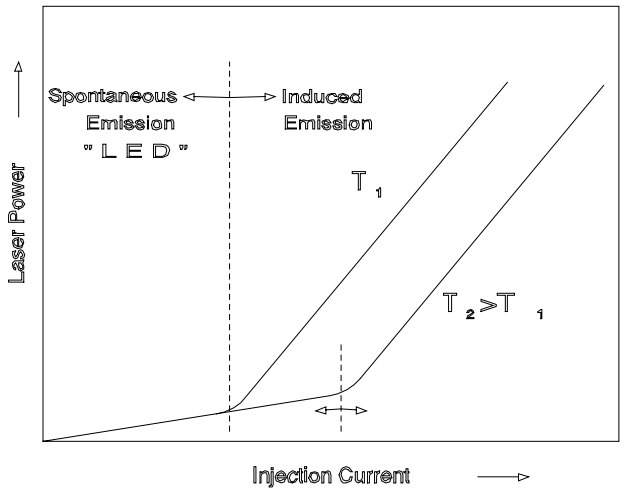

Fig. 40: Laser power versus injection current with the temperature T as parameter

The wavelength of the laser diode depends on the temperature T and the injection current I in the following way:

$$\lambda(T,I) = \lambda(T_0,I_0) + \alpha_T(T-T_0) + \alpha(I-I_0) + \alpha_T^2(T-T_0)^2 + \alpha_I^2(I-I_0)^2 + ... \alpha_T^n(T-T_0)^n + \alpha_I^n(I-I_0)^n$$

$\lambda(T_0, I_0)$ is a known wavelength at T_0 and I_0.. Generally it is sufficient to consider only the linear terms. For a precision of $\delta\lambda/\lambda < 10^{-6}$ the quadratic terms have to be respected. The equation is valid within a jump-free range. The requirement $\lambda(T,I) = const. = \lambda_c$ provides directly:

$$I = \frac{(\lambda_c - \lambda_0)}{\alpha_I} - \frac{\alpha_T}{\alpha_I}(T-T_0)$$

One gets a dependence as shown in Fig. 41

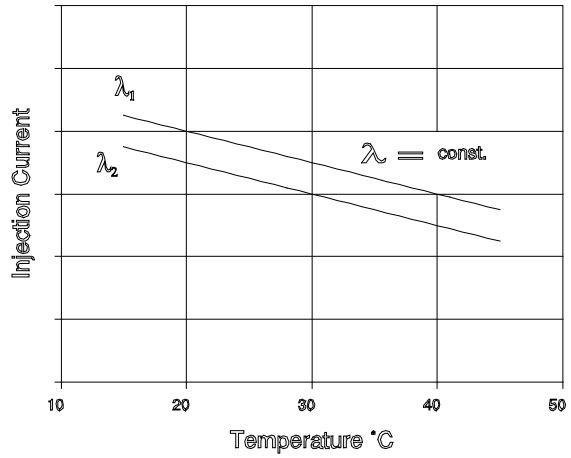

Fig. 41: Injection current as a function of the temperature for constant wavelength

2.8.8 Optical power

In regard to „classical“ lasers the light of a diode laser contains a remarkable high fraction of non-coherent „LED“ radiation. For currents underneath the laser threshold the spontaneous emission is dominant. Stimulated emission is responsible for the strong increase above the laser threshold. The threshold current can be determined by the point of intersection of the extrapolated characteristic lines of the initial and of the lasing working mode. The rounding off of the characteristic line is the result of spontaneous emission. It also is the cause for the oscillation of several modes next to the threshold. At higher currents the mode spectrum becomes more and more clean.

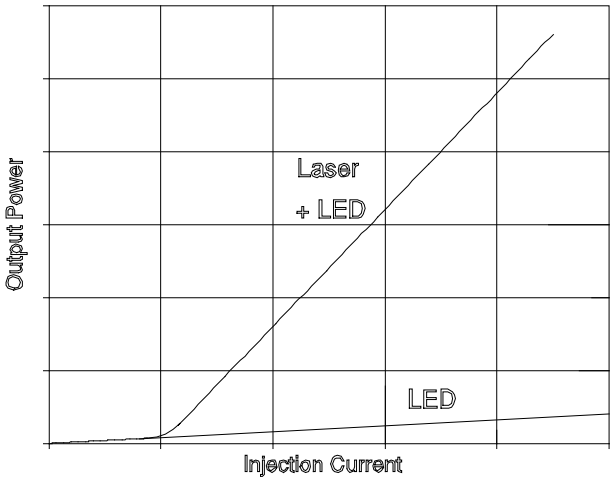

Fig. 42: Output power of the laser diode as a function of the injection current

2.8.9 Detectors, properties and range of applications

Semiconductor pn-transitions with a band gap of E_g are suitable for the detection of optical radiation if the energy E_p of the photons is equal or greater than the band gap.

$$E_p = \hbar\omega \geq E_g$$

In this case an arriving photon can stimulate an electron to pass from the valence band to the conduction band. (Fig. 43).

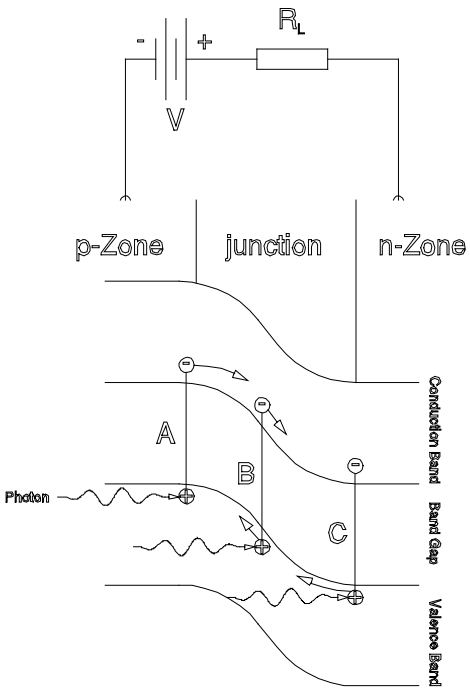

Fig. 43: Absorption of a photon with subsequent transition of the stimulated electron from the valence band to the conduction band

Here three types of events are possible:

A An electron of the valence band in the p-zone is stimulated and enters the p-zone of the conduction band. Because of the external electric field due to the voltage V it will diffuse through the barrier layer into the n-zone and contributes to the external current passing the resistor R_L unless it recombines in the p-zone.

B If an electron of the barrier layer is hit by a photon the hole of the barrier layer will migrate into the p-zone and the electron into the n-zone. The drift of both charges through the barrier layer causes a current impulse. The duration of the impulse depends on the drift speed and on the length of the barrier layer.

C The case is similar to case A. The hole migrates due to the presence of the external field into the p-zone or recombines in the n-zone.

Only electrons which are in the barrier layer (case B) or near the boundary of the barrier layer (area of diffusion, case A and C) contribute to the external current due to stimulation by photons. All others will recombine within their area. In the utmost case one elementary charge q can be created for each incoming photon. As already mentioned, not every photon will create in the average a current impulse. In this context the production rate G, leading to an average current $\langle i_{Ph} \rangle$ is defined as follows:

$$\langle i_{Ph} \rangle = q \cdot G$$

At a light energy of P_0 a number of $\frac{P_o}{\hbar\omega}$ photons will hit the detector as $\hbar\omega$ is just the energy of one photon. But only that fraction of photons is converted into current pulses which is absorbed in the barrier layer. This fraction may be called $\eta \cdot P_0$, where η is called quantum efficiency. The number of generated current pulses or the production rate will be

$$G = \frac{\eta}{\hbar\omega} \cdot P_0$$

and the average photo current:

$$\langle i_{Ph} \rangle = \frac{\eta \cdot q}{\hbar\omega} \cdot P_0$$

Because of processes which are typical for semiconductors there is already a current flowing even if there are no photons entering the detector. This current is called „dark“ current and has four reasons:

1. diffusion current, it is created because of statistical oscillations of the charge carriers within the diffusion area

2. regeneration or recombination current, it is generated by random generation and annihilation of holes

3. surface currents, which are hardly avoidable since the ideal insulator does not exist

4. avalanche currents are flows of electrons which appear at high electric field strengths, if, for example, a high voltage is applied to the photodiode

All these effects contribute to the dark current i_D in a way that finally the characteristic line of the diode can be expressed as follows:

$$i = i_s \left(e^{\frac{q \cdot U_D}{kT}} - 1 \right) - \langle i_{Ph} \rangle = i_D - \langle i_{Ph} \rangle$$

This current i passes the load resistor R_L and provokes the voltage drop U_a, which represents the signal.

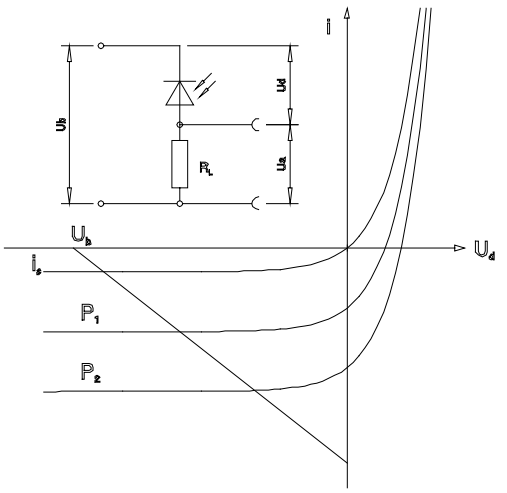

Fig. 44: Characteristic line of a photodiode in the photoconductive mode

$$i = i_s\left(e^{\frac{q}{kT}U_d} - 1\right) - \left\langle i_{Ph}\right\rangle = \frac{U_a}{R_L}$$

A good detector of optical communication technology is characterised by the fact that it is very fast (up to the GHz range) and that it has a high quantum efficiency which means that it is very sensitive. Depending on the wavelength range which has to be covered by the detector one uses silicon or germanium semiconductor material for the construction of the detectors.

2.8.10 Germanium and silicon PIN-diodes

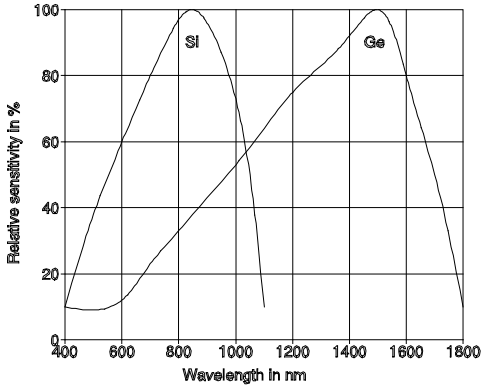

Fig. 45: Relative sensibility for Si und Ge photodetector

To have absorption of a photon at all its energy has to fit into the band structure of the material under consideration. From the condition

$$E_{ph} = \hbar\omega = h\nu = \frac{hc}{\lambda} \geq E_G$$

one recognises that for large wavelengths the energy of the photon may no more be sufficient „ to lift“ the electron in a way that it passes the band gap. For smaller wavelengths one has to respect that the conduction band and also the valence band have upper edges which is followed by a band gap. Photon energies which pass the upper limit of the conduction band can no more be absorbed. The wavelength of the applied light source decides which detector material is to be used. For wavelengths above 1 µm up to 1.5 µm Germanium is recommended. Underneath these values Silicon detectors are used. In the present experiment a laser diode of 810 nm wavelength is applied. Therefore a silicon detector is used. To get a high quantum efficiency not a PN but a PIN detector has been chosen.

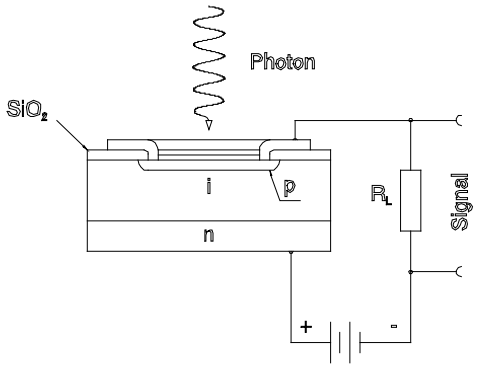

Fig. 46: Construction of a PIN detector

Contrary to a detector with a simple pn-layer this type of detector has an intrinsic conducting layer inserted in between the p-and n-layer. Therefore the name PIN-diode. The reason for this is to enlarge the barrier layer which increases the probability of absorbtion of a photon and the generation of a current impulse, e.g. the quantum efficiency. The quantum efficiency for such an arrangement is:

$$\eta = (1-R)\left(1-e^{-\alpha d}\right)e^{-\alpha d_p}$$

R is the Fresnel reflection at the Si or Ge surface which is hit by the photons, α is the coefficient of absorption, d the thickness of the intrinsic zone and d_p the thickness of the p-layer. By attachment of a reflex reducing layer on the upper side of the p-layer R can get a value of less than 1%. Since αd_p is anyhow <<1, the thickness of the intrinsic layer should be chosen as large as possible. The consequence of this is that the drift time rises and the limiting frequency of the detector is reduced. In so far a compromise between high quantum efficiency and high limiting frequency has to be made. In this experiment a PIN-Si-photo diode, type BPX61 is used. It has the following characteristic values:

Quantum efficiency η at 850 nm	90 %
Rising time $\tau_r = 2.2 \cdot R_L C_j$ 10%-90% at R_L= 50Ω and U_d=10V	1.7 ns
Capacity C_j at U_d =	
0 V	73 pF
1 V	38 pF
10 V	15 pF
dark current i_d at U_d = 10V	2 nA
Photosensitivity at U_d = 5V	70 nA/lx

3 Index of literature

[1] K. J. Ebeling, Integrierte Optoelektronik, 1989

Springer Verlag, Berlin

[2] H.-G. Unger, Optische Nachrichtentechnik, Bd. 1,1993

Hüthig Buch Verlag GmbH, Heidelberg

[3] Jahnke-Emde-Lösch; Tables of higher functions, 1966

B.G. Teubner Verlagsgesellschaft, Stuttgart

[4] K.J. Ebeling, Integrierte Optoelektronik,

Springer Verlag ISBN 3-540-51300-0,(1989).

[5] Alonso-Finn, Physik III

Inter European Editions B.V., ISBN 0-201-00276-0, (1974).

[6] G. Joos, Lehrbuch der theoretischen Physik

Akademische Verlagsgesellschaft m.b.H. (1959).

[7] Stephen Gasiorowicz, Quantenphysik

R. Oldenbourg Verlag München Wien 1977,

[8] W. Finkelnburg, Einführung in die Atomphysik

Springer-Verlag Berlin Heidelberg New York 1967

4 Unpacking

The experimental system EXP 12 Glass Fibre Optics comes packed in a storage and transportation case. All components are placed in a foam padding as shown below.

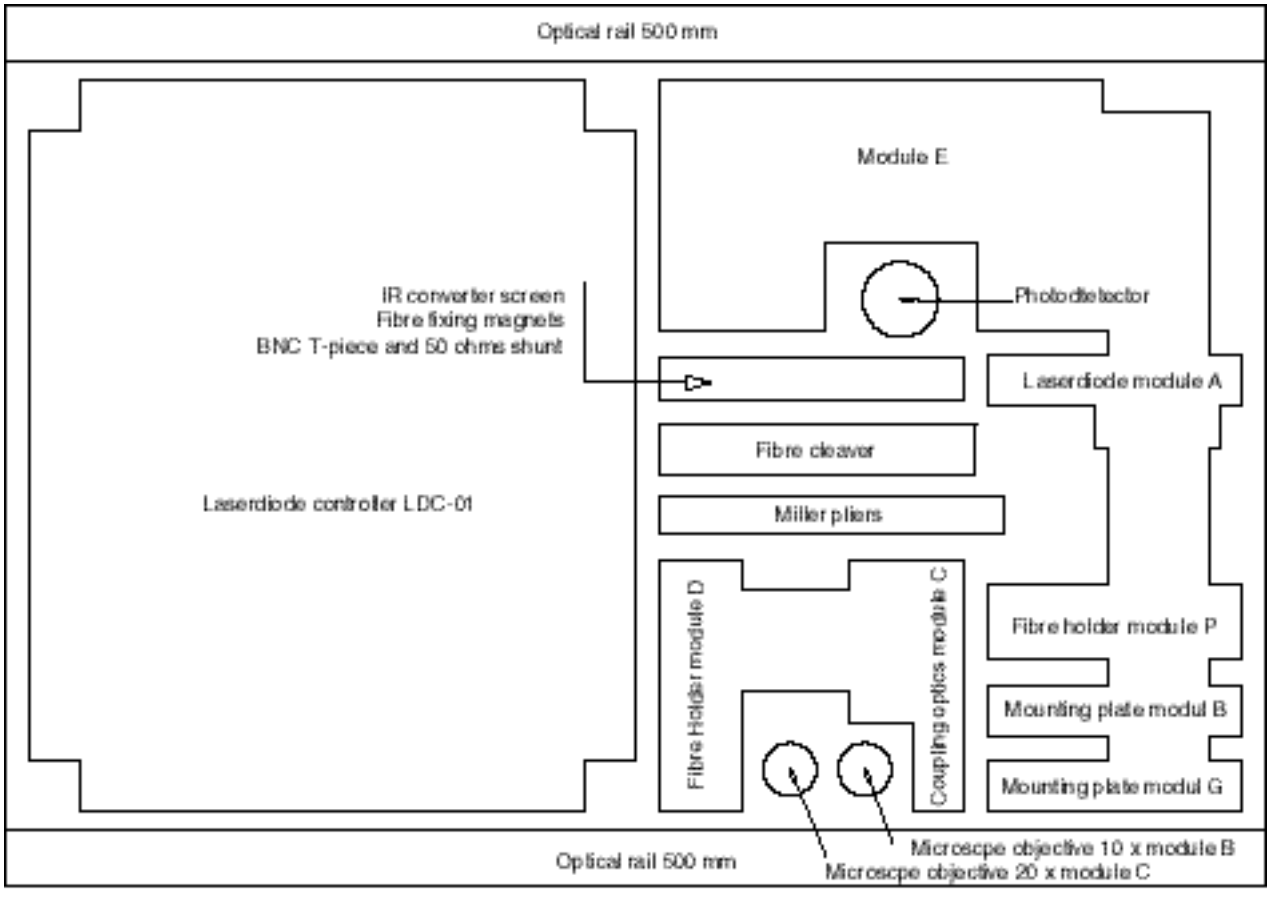

Fig. 47: Before using the components screw the microscope objective 10 x into the mounting plate of module B and the 20 x into the holder for the coupling optics module C.

5 Preparing the fibre

Before using the fibre it has to be prepared in such a way that the input as well as output faces are perpendicular as well as of best optical quality. This is achieved by using a fibre cleaver and breaker. To do so first of all the plastic coating has to be removed by means of the so called Miller's pliers.

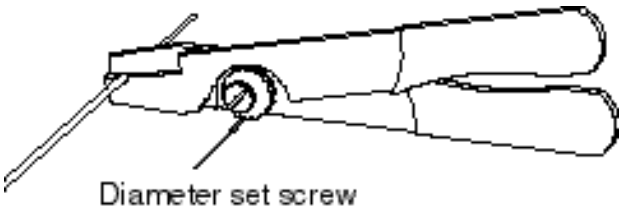

Fig. 48: Miller's pliers

The pliers have to be adjusted in such a way that the closed pliers do not scratch the glass of the fibre by removing the plastic cover. This is be done by adjusting the diameter set screw.

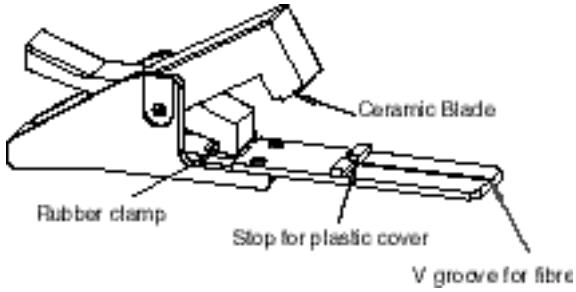

Fig. 49: Fibre cleaver and breaker

The fibre with removed plastic coating is inserted in such a way that the remained plastic coating stops at the stopper (Fig. 49) and the coating free part inside the rubber clamp.

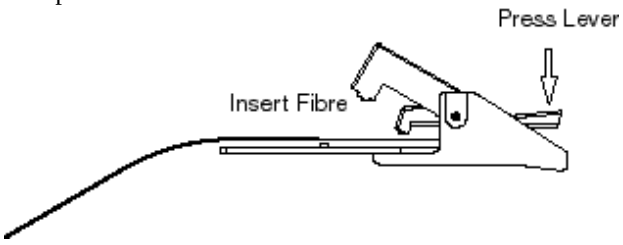

Fig. 50: First phase

Press the lever as shown in Fig. 50 and insert the fibre.

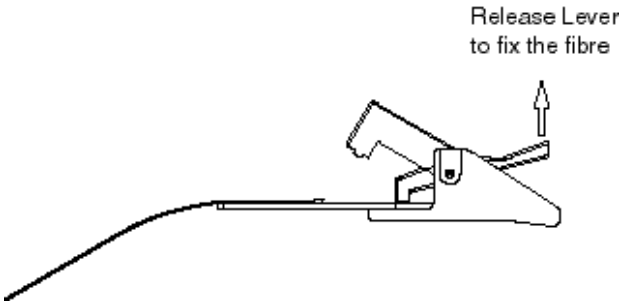

Fig. 51: Second phase

Release the lever to fix the fibre by means of the rubber clamp.

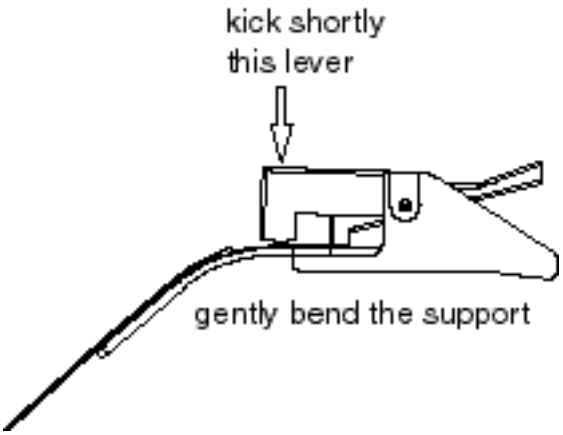

Fig. 52: Third phase

Gently bend the support and kick shortly the ceramic blade of the cutter lever onto the fibre. The fibre will break.

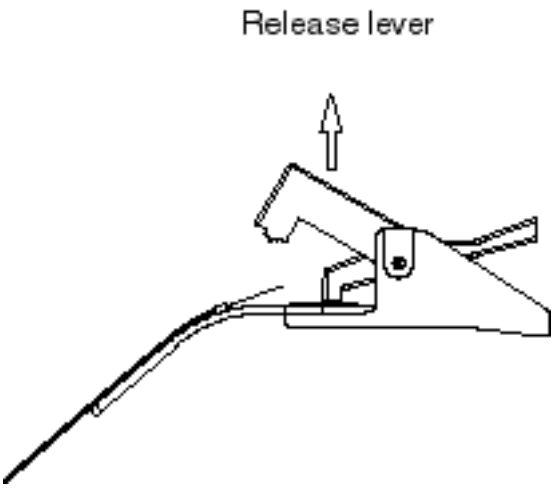

Fig. 53: Final phase

Remove the ready fibre from the cleaver.

Attention: Remove the rest of the fibre and deposit in a closed box or container to avoid that these parts may enter and injure the human body.

6 Experiments

6.1 Experimental set-up

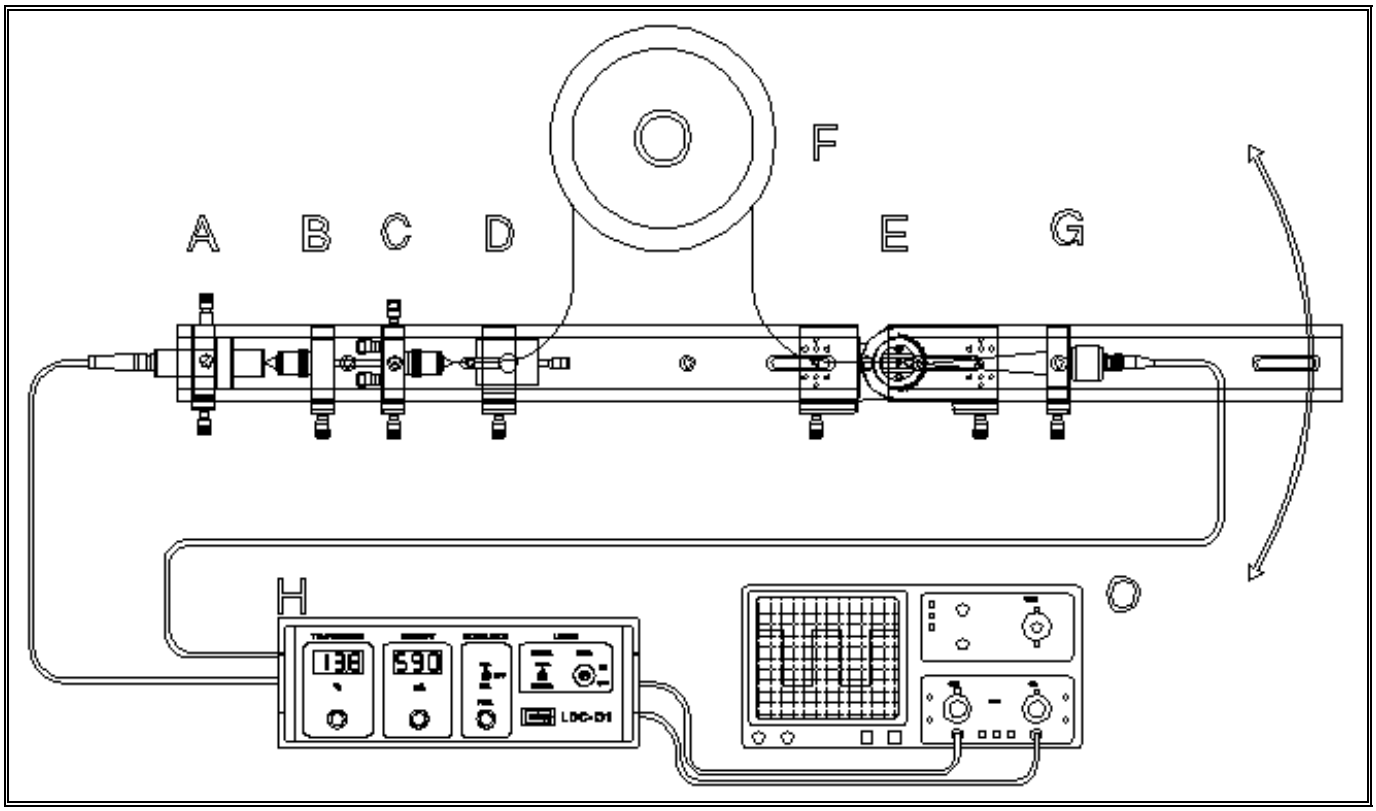

Fig. 54: Experimental set-up with monomode fibre

This set-up has been made with a monomode fibre. Because of didactic reasons a fibre without protective coating has been selected. The connection of the fibre with module D is done in the following way:

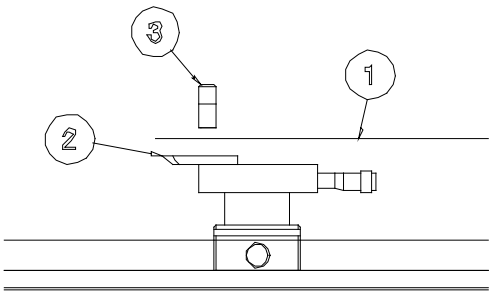

Fig. 55: Mounting the plug connection to module D

The cut and cleaved fibre (1) is put into the groove of holder 2 and carefully fixed with the magnet (3).

Module A : The laser diode in its housing is mounted on a XY-fine adjustment. A Peltier cooler and a thermistor for measuring the laser diode temperature are incorporated in the housing. The laser diode emits a maximum power of 50 mW.

Module B: A microscope objective collimates the laser diode radiation. The objective is screwed into the mounting plate that it can easily be taken away from the plate holder and exchanged for another one.

Module C: Basically the same arrangement as module B but with a fine adjustment holder with four axis XY, θ and ϕ and an objective of smaller focal distance to focus the collimated laser diode radiation in such a way that an effective coupling to the fibre is ensured. Purposely a beam shaping of the laser diode radiation has been omitted to simplify the entrance into the experiment.

Module D: Before starting the experiment the prepared fibre is mounted to the module D. The fibre holder is mounted on a stage with linear displacement in the direction of the beam.

Module F: 100 m monomode fibre are coiled up on a drum. Of course also multimode fibres can be used, which make alignment much more easy.

Module E: On a hinged joined angle connector the second fibre holder is mounted, but without a linear stage. This device allows to measure the angle dependent output power of the fibre.

Module G: This module consists of the detector with a PIN photodiode. The connection to the preamplifier of the control unit LDC01 is made by a BNC cable. The inner pin of the BNC plug is in contact with the anode of the photo.

A description of the control unit LDC01 is attached as appendix.

6.2 Properties of the laser diode used

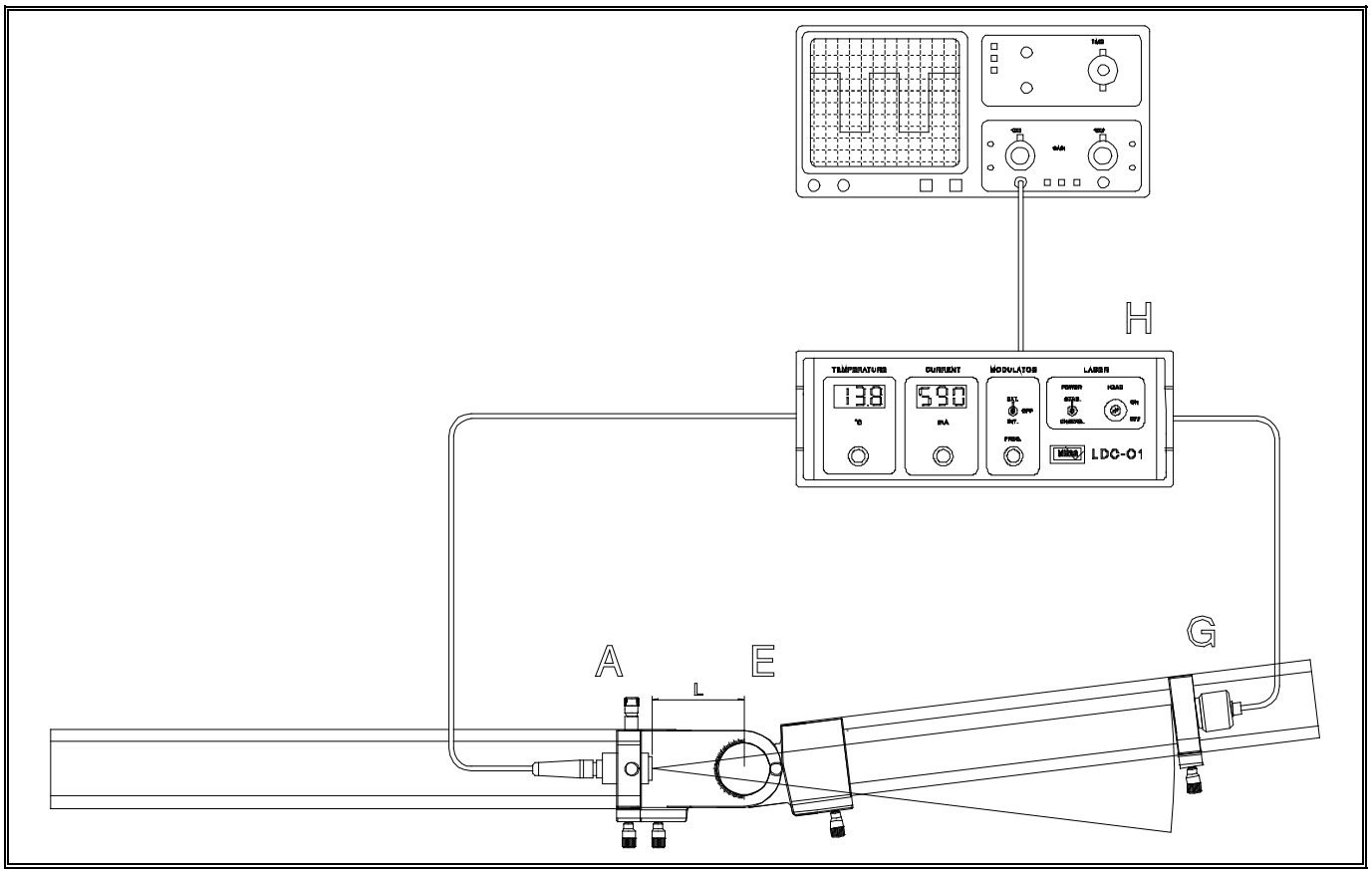

6.2.1 Spatial intensity distribution

By means of the above shown set-up the intensity distribution of the laser diode is measured. For this reason the laser diode module is set quite near to the rotation joint so that the unavoidable distance L from the axis of the rotation joint is a minimum. To measure the intensity distribution as a function of the angle with reference to another axis of the laser diode, the latter one can be rotated in its holder. The lateral screw (M3-screw) is released at the holder for this reason and the laser diode is turned into the desired position. It gives a sense to measure the intensity distribution once in direction of the greatest divergence and under 90^0 with respect to this direction. To eliminate the influence of environmental light from the detector the laser diode should be modulated. Therefore the modulation switch on the front panel is switched to the „on“ position. By means of the control button for the modulation frequency a frequency which is not too high will be selected in a way that proper rectangular signals can be observed. The output of the photo diode amplifier of the LDC01 control unit is connected to an oscilloscope. This is switched to the „AC“ mode. Our object of observation is exclusively the amplitude. In that way all environmental disturbances can be eliminated. With the same set-up, but the detector under 0^0 to the laser diode, the output power is measured as a function of the injection current and the temperature of the laser diode. Attention has to be paid to the fact that the detector does not approach saturation, which can be assured by choosing the distance to the laser diode in an appropriate manner. If a monochromator is available (can be ordered optionally), the dependence of the wavelength on the temperature and on the injection current can be measured.

6.2.2 Modulation behaviour of the laser diode

The control unit LDC01 has a modulation input to which a signal generator can be connected. That way the injection current can be modulated by any type of signal.
The signal generator should have an adjustable off-set to get the working point in the midst of the characteristic line. As signal generator any source of signals can be used, also sources of digital signals, provided they have the required input voltage level (more details in the instruction manual of the control unit).

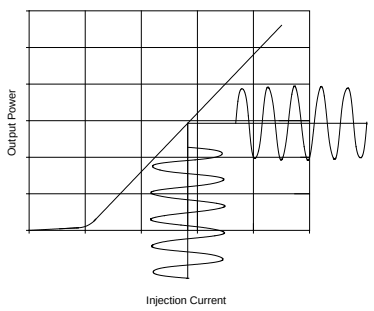

6.3 Measurements with the fibre

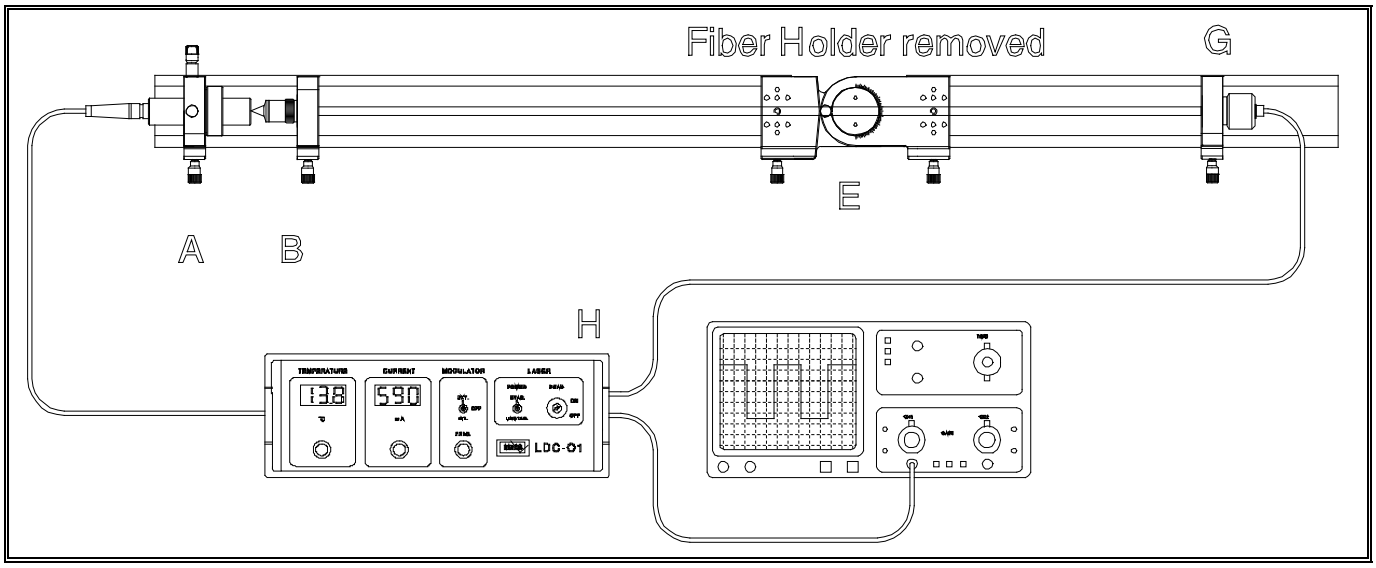

Aligning the diodelaser

Before we take off with the measurements we have to define the optical axis of the set-up. This is done with the help of an oscilloscope. Again the injection current is modulated so that we can see rectangular pulses on the oscilloscope. The collimator (Module B) is brought at such a position to the laser diode that a nearly parallel laser beam is formed. By means of the XY-displacement screws of module A the laser beam is then centralised on the detector. This can be checked by looking for the maximum signal on the oscilloscope. Precaution has to be taken that the detector does not reach saturation. Eventually the injection current has to be reduced by a suitable amount. The next step is to bring the coupling optics (Module C) into the set-up.

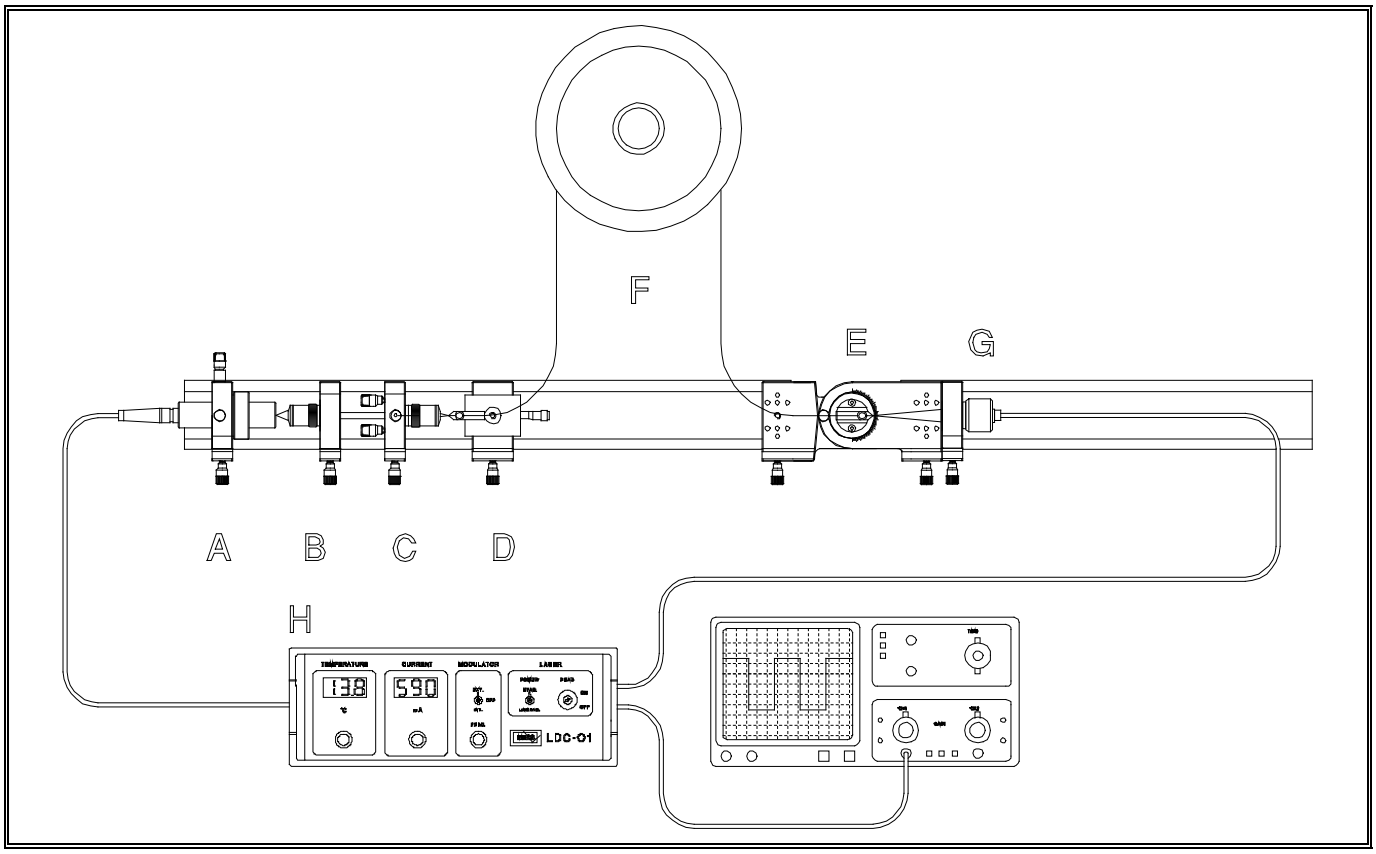

Insert of Module C

The distance of module C to B is more or less arbitrary since the laser beam is nearly parallel. 50 mm are recommended. Now the fibre adjustment holder (Module D, without fibre) is put on the rail at a distance of about 10 mm from module C. The fibre is then carefully mounted to the fibre adjustment holder and inserted. The laser diode is switched to maximum injection current and the internal modulation is „on“. The detector is fixed to the holder plate F vis a vis of the fibre exit. If the amplifier of the control unit and the oscilloscope are set to highest amplification one already detects modulated laser light at the exit of the fibre. Now the fibre has to be adjusted. While observing the amplitude on the oscilloscope one turns gently the XY and θϕ adjustment screws of the adjustment holder. If there is no further increase in the amplitude the distance between fibre and coupling optics will be changed by acting on the linear displacement of the sliding mount. In the new position the adjustment screws are readjusted. Since the amplitude increases continuously the amplification of the oscilloscope has to be reduced accordingly. At a certain state of adjustment the injection current has to be reduced since meanwhile so much power is coupled to the fibre that the detector approaches saturation. By means of the IR conversion card one can now observe the outgoing radiation if the room is sufficiently darkened. The previous adjustment steps are repeated until no more power increase is observed. The set-up is now well prepared for the following measurements.

6.3.1 Numerical aperture

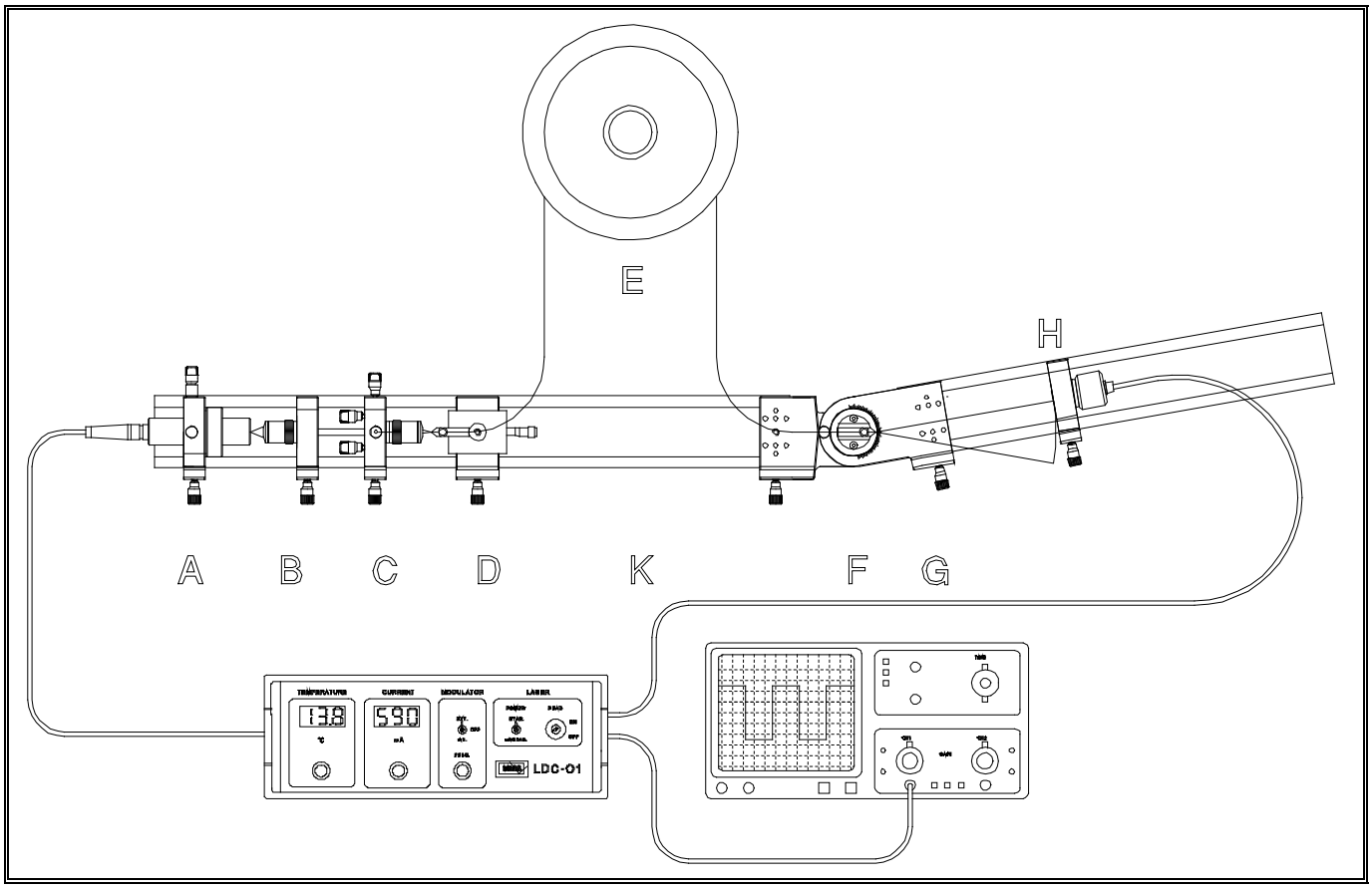

The detector is taken off from holder F and inserted into holder H. The holder H is positioned on the right rail at a selected distance to holder F. The smallest distance is predetermined by the rotation joint. The power is measured for different angles. Here, too, we use modulated light to eliminate the influence of environmental disturbances.

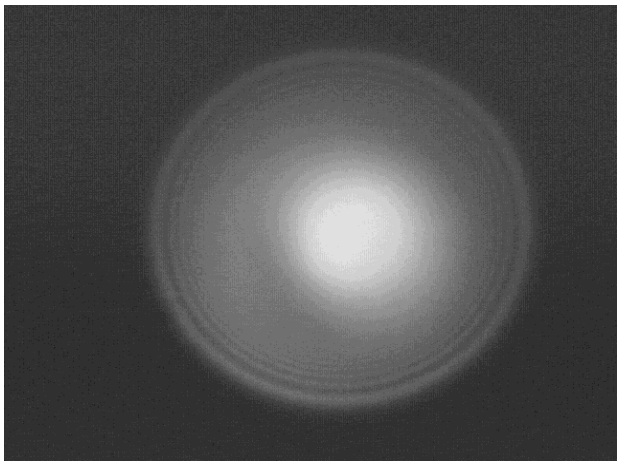

In determining the numerical aperture we will meet some physical effects which make the interpretation of the measured values a bit difficult. We are speaking about the cladding waves which leave the fibre together with the core waves simulating an aperture which is just too high. At larger distances of the detector this influence is remarkably reduced. The picture shown in the left was taken with a simple CCD camera during a measurement. It is clearly to see that next to the central LP_{01}-mode a rather appreciable intensity leaves the fibre via the cladding. It is this intensity which eventually may simulate a too high numerical aperture. With the help of this simple but impressive technology these problems can be bypassed. For completeness reasons it must be mentioned that these cladding modes can also be eliminated by using a „mode stripper“. This can be achieved by removing the protective coating of the fibre near the end of the fibre and bending it over an arc of about 7 cm within a liquid which has a similar refractive index as the cladding. (for example oil of paraffin). By this method the cladding modes are going to leave the fibre before they can falsify the measurements.

6.3.2 Transit time effects

Another very interesting experiment is the measurement of the transit time of light through the fibre. The set-up is modified so that the detector is again next to the end of the fibre in holder E.

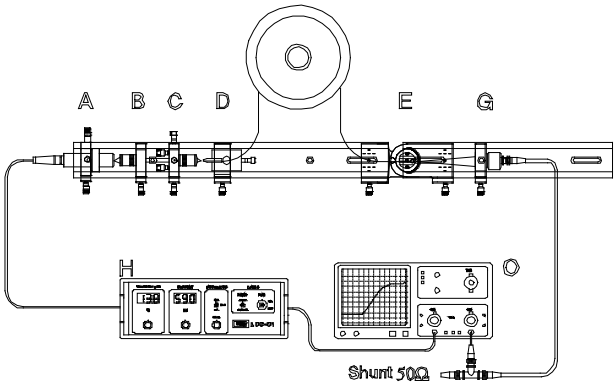

Fig. 56: Use of the 50 Ohms shunt resistor

The detector is connected directly to the oscilloscope. To reduce the rise time of the signal a 50Ω resistor is used as shunt. The second channel is connected to the monitor exit of the injection current at the control unit LDC01. For an appropriate set of the time base one gets curve A.

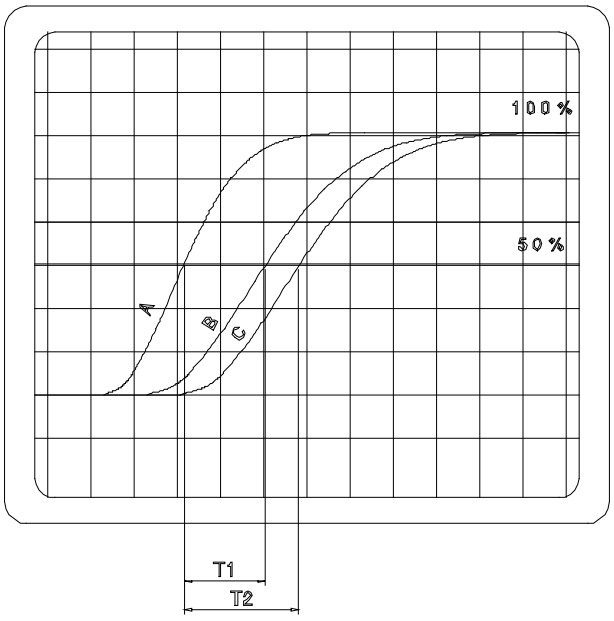

The fibre is now eliminated from the set-up by taking off the mounted plug connections from the holders. (Attention! Put the fibre ends at a safe place)

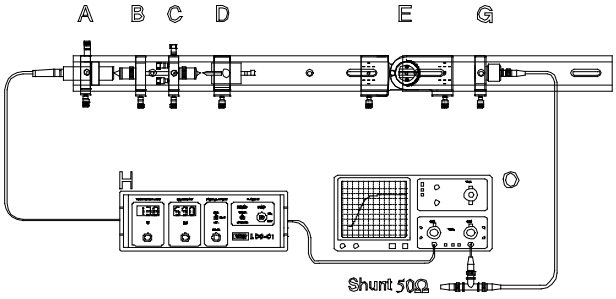

Fig. 57: Measuring the system delay

Curve B is represented and the time difference T_1 at 50 % of the rise time is measured. The time T_1 represents all transit time delays of the system without fibre. Then the fibre is reinserted and adjusted to maximum power. Next we are going to find curve C and time T_2 . The time T_2 contains the transit time delays of the system and the transit time of the light through the fibre. The order of magnitude of the transit time through the fibre can be estimated as follows:

$$\tau_{Light} = \frac{L}{c} \cdot n_{eff} = \frac{100}{3 \cdot 10^8} \cdot 1.45 \approx 0.5 \mu s$$

6.4 Set-up of a data segment

The previous experiments dealt with the modulation of the light of a laser diode on one side and with the coupling of light on the other. For the transmission rectangular signals were used to determine the fibre parameters numerical aperture and transit time. The set-up of a data segment requires additionally the following:

1. Selection of an appropriate signal source for the input of the control unit. Here the required voltage levels have to be minded. The limiting frequency of 1 MHz for sine wave signals should not be passed.
2. The signal source has to have an „off-set“ button to enable a proper choice of the working point on the characteristic line of the laser diode.
3. The detector can be connected to the measuring instrument by passing over the amplifier of the control unit or directly. In this case a resistor has to be connected in parallel to the detector to get the necessary rise time.
4. With the help of the oscilloscope the injection current is monitored. It informs about the sensible use of the characteristic line of the laser diode.

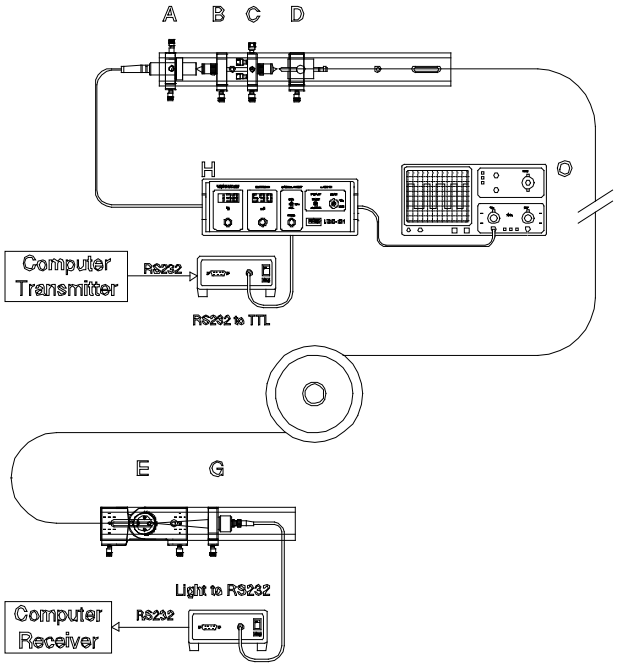

Fig. 58: Possible use for PC data transmission

7 Mathematical Appendix

7.1 The modified Hankel-function

The Hankel-function itself results in complex values. By rotation of the coordinate system by 90 degree the values of the Hankel-function needed for the description of the physical situation become real. That means the imaginary axis has been rotated into the real axis.

$$I_p(\mathrm{v}) = e^{-p\frac{\pi}{2}i} \cdot J_p\left(\mathrm{v} \cdot e^{\frac{\pi}{2}i}\right) = \left(\frac{\mathrm{v}}{2}\right)^p \cdot \sum_{k=0}^{\infty} \frac{1}{k! \cdot \prod(p+k+1)} \left(\frac{\mathrm{v}}{2}\right)^{2k}$$

$$K_p(\mathrm{v}) = \frac{\pi \cdot i}{2} e^{p\frac{\pi}{2}i} H_p^{(1)}\left(\mathrm{v} \cdot e^{\frac{\pi}{2}i}\right)$$

$$K_p(\mathrm{v}) = (-1)^{p+1} I_p(\mathrm{v}) \cdot \left(C + \ln\left(\frac{\mathrm{v}}{2}\right)\right) + \frac{(-1)^p}{2} \sum_{k=0}^{\infty} \frac{1}{k!(p+k)!} \cdot \left(\frac{\mathrm{v}}{2}\right)^{p+2k} \cdot \left(\sum_{l=1}^{k} \frac{1}{l} + \sum_{l=1}^{p+k} \frac{1}{l}\right)$$
$$+ \frac{1}{2} \sum_{k=0}^{p-1} \frac{(-1)^k (p-k-1)!}{k!} \left(\frac{\mathrm{v}}{2}\right)^{2k-p}$$

For the derivation with respect to ∂v the following relation is valid:

$$\frac{\partial K_p(\mathrm{v})}{\partial \mathrm{v}} = K_p' = -\frac{1}{2}\left(K_{p-1} + K_{p+1}\right)$$

$$\frac{\partial K_0'}{\partial \mathrm{v}} = -K_1$$

Recurrence formula:

$$K_{p-1}(\mathrm{v}) - K_{p+1}(\mathrm{v}) = -\frac{2p}{\mathrm{v}} K_p(\mathrm{v})$$

For the used abbreviation X_p we get by using the differentiation and recurrence formula:

$$X_p = \frac{K_p'(\mathrm{v})}{\mathrm{v} \cdot K_p(\mathrm{v})} = -\frac{1}{2\mathrm{v}} \frac{K_{p-1}(\mathrm{v}) + K_{p+1}(\mathrm{v})}{K_p(\mathrm{v})} = -\frac{1}{2\mathrm{v}} \frac{-\frac{2p}{\mathrm{v}} K_p(\mathrm{v}) + K_{p+1}(\mathrm{v}) + K_{p+1}(\mathrm{v})}{K_p(\mathrm{v})}$$

$$= \frac{1}{\mathrm{v}} \frac{\frac{p}{\mathrm{v}} K_p(\mathrm{v}) - K_{p+1}(\mathrm{v})}{K_p(\mathrm{v})} = -\frac{K_{p+1}(\mathrm{v})}{\mathrm{v} K_p(\mathrm{v})} + \frac{p}{\mathrm{v}^2}$$

or:

$$X_p = \frac{K_p'(\mathrm{v})}{\mathrm{v} \cdot K_p(\mathrm{v})} = -\frac{1}{2\mathrm{v}} \frac{K_{p-1}(\mathrm{v}) + K_{p+1}(\mathrm{v})}{K_p(\mathrm{v})} = -\frac{1}{2\mathrm{v}} \frac{K_{p-1}(\mathrm{v}) + \frac{2p}{\mathrm{v}} K_p(\mathrm{v}) + K_{p-1}(\mathrm{v})}{K_p(\mathrm{v})}$$

$$= -\frac{1}{\mathrm{v}} \frac{K_{p-1}(\mathrm{v}) + \frac{p}{\mathrm{v}} K_p(\mathrm{v})}{K_p(\mathrm{v})} = -\frac{K_{p-1}(\mathrm{v})}{\mathrm{v} K_p(\mathrm{v})} - \frac{p}{\mathrm{v}^2}$$

and generalised:

$$X_p = -\frac{K_{p\pm1}(\mathrm{v})}{\mathrm{v}K_p(\mathrm{v})} \pm \frac{p}{\mathrm{v}^2}$$

For v << *1* the following relations are valid:

$$K_0(\mathrm{v}) \approx \ln\left(\frac{2}{e^C \cdot \mathrm{v}}\right)$$

$$K(\mathrm{v})_{p,p>0} \approx \frac{1}{2}\,p!\left(\frac{\mathrm{v}}{2}\right)^{-p}$$

$$X_p = -\frac{K_{p\pm1}(\mathrm{v})}{\mathrm{v}K_p(\mathrm{v})} \pm \frac{p}{\mathrm{v}^2} \Rightarrow$$

$$p = 1 \Rightarrow X_1 = -\frac{K_o}{\mathrm{v}K_1} - \frac{1}{\mathrm{v}^2} = \ln\left(\frac{2}{e^C \cdot \mathrm{v}}\right) - \frac{1}{\mathrm{v}^2} = -\frac{1}{\mathrm{v}^2} - \ln\frac{\mathrm{v}}{2} - C$$

$$p \geq 2 \Rightarrow X_p = -\frac{K_{p-1}(\mathrm{v})}{\mathrm{v}K_p(\mathrm{v})} - \frac{p}{\mathrm{v}^2} = -\frac{(p-1)!\left(\frac{\mathrm{v}}{2}\right)^{-p+1}}{\mathrm{v}p!\left(\frac{\mathrm{v}}{2}\right)^{-p}} - \frac{p}{\mathrm{v}^2} = -\frac{1}{2\cdot(p-1)\cdot} - \frac{p}{\mathrm{v}^2}$$

7.2 Calculation of the constants C_E,C_H,D_E and D_H using the continuity condition

The solutions of the wave equation are substituted into the equations (2.5.6), (2.5.7) and (2.5.8).

$$E_{\phi k} = -\frac{i}{k_k^2}\left[\frac{ip\beta}{a}E_{zk} - \mu_0\omega\frac{\partial H_{zk}}{\partial r}\right] = \frac{p\beta}{k_k^2 a}C_E J_p e^{ip\phi} + \frac{i\mu_0\omega}{k_k^2}C_H\frac{\partial J_p}{\partial r}e^{-ip\phi}$$

$$E_{\phi m} = -\frac{i}{k_m^2}\left[\frac{ip\beta}{a}E_{zm} - \mu_0\omega\frac{\partial H_{zm}}{\partial r}\right] = \frac{p\beta}{k_m^2 a}D_E K_p e^{ip\phi} + \frac{i\mu_0\omega}{k_m^2}D_H\frac{\partial K_p}{\partial r}e^{-ip\phi}$$

$$H_{\phi k} = -\frac{i}{k_k^2}\left[\omega\varepsilon_0 n_k^2\frac{\partial E_{zk}}{\partial r} - \frac{ip\beta}{a}H_{zk}\right] = -\frac{i\omega\varepsilon_0 n_k^2}{k_k^2}C_E\frac{\partial J_p}{\partial r}e^{ip\phi} - \frac{p\beta}{ak_k^2}C_H J_p e^{-ip\phi}$$

$$H_{\phi m} = -\frac{i}{k_m^2}\left[\omega\varepsilon_0 n_m^2\frac{\partial E_{zm}}{\partial r} - \frac{ip\beta}{a}H_{zm}\right] = -\frac{i\omega\varepsilon_0 n_m^2}{k_m^2}D_E\frac{\partial K_p}{\partial r}e^{ip\phi} - \frac{p\beta}{ak_m^2}D_H K_p e^{-ip\phi}$$

We now use the definition for u and v :

$$E_{zk} = C_E J_p \cdot e^{ip\phi}$$

$$E_{zm} = D_E K_p \cdot e^{ip\phi}$$

$$E_{\phi k} = \frac{p\beta a}{u^2}C_E J_p \cdot e^{ip\phi} + \frac{i\mu_0\omega a^2}{u^2}C_H J_p' \cdot e^{-ip\phi}$$

$$E_{\phi m} = -\frac{p\beta a}{\mathrm{v}^2}D_E K_p \cdot e^{ip\phi} - \frac{i\mu_0\omega a^2}{\mathrm{v}^2}D_H K_p' \cdot e^{-ip\phi}$$

$$H_{zk} = C_H J_p \cdot e^{-ip\phi};\; H_{zm} = D_H K_p \cdot e^{-ip\phi}$$

$$H_{\phi k} = -\frac{i\omega\varepsilon_0 a^2 n_k^2}{u^2}C_E J_p' \cdot e^{ip\phi} - \frac{p\beta a}{u^2}C_H J_p \cdot e^{-ip\phi}$$

$$H_{\phi m} = \frac{i\omega\varepsilon_0 a^2 n_m^2}{\mathrm{v}^2}D_E K_p' \cdot e^{ip\phi} + \frac{p\beta a}{\mathrm{v}^2}D_H K_p e^{-ip\phi}$$

The continuity relation for the radial field components:

$$E_{\phi k} - E_{\phi m} = \frac{p\beta a}{u^2} C_E J_p \cdot e^{ip\phi} + \frac{i\mu_0 \omega a^2}{u^2} C_H J'_p \cdot e^{-ip\phi} + \frac{p\beta a}{v^2} D_E K_p \cdot e^{ip\phi} + \frac{i\mu_0 \omega a^2}{v^2} D_H K'_p \cdot e^{-ip\phi} = 0$$

$$H_{\phi k} - H_{\phi m} = + \frac{i\omega\varepsilon_0 a^2 n_k^2}{u^2} C_E J'_p \cdot e^{ip\phi} - \frac{p\beta a}{u^2} C_H J_p \cdot e^{-ip\phi} + \frac{i\omega\varepsilon_0 a^2 n_m^2}{v^2} D_E K'_p \cdot e^{ip\phi} - \frac{p\beta a}{v^2} D_H K_p e^{-ip\phi} = 0$$

The complete continuity relation written in matrix form:

$$\mathrm{A_{ik}} \cdot \begin{bmatrix} C_E \\ C_H \\ D_E \\ D_H \end{bmatrix} = \begin{bmatrix} J_p \cdot e^{ip\phi} & 0 & -K_p \cdot e^{ip\phi} & 0 \\ 0 & J_p \cdot e^{-ip\phi} & 0 & -K_p \cdot e^{-ip\phi} \\ \frac{p\beta a}{u^2} J_p \cdot e^{ip\phi} & \frac{i\mu_0 \omega a^2}{u^2} J'_p \cdot e^{-ip\phi} & \frac{p\beta a}{v^2} K_p \cdot e^{ip\phi} & \frac{i\mu_0 \omega a^2}{v^2} K'_p \cdot e^{-ip\phi} \\ \frac{i\omega\varepsilon_0 a^2 n_k^2}{u^2} J'_p \cdot e^{ip\phi} & -\frac{p\beta a}{u^2} J_p \cdot e^{-ip\phi} & \frac{i\omega\varepsilon_0 a^2 n_m^2}{v^2} K'_p \cdot e^{ip\phi} & -\frac{p\beta a}{v^2} K_p e^{-ip\phi} \end{bmatrix} \cdot \begin{bmatrix} C_E \\ C_H \\ D_E \\ D_H \end{bmatrix} = \begin{bmatrix} 0 \\ 0 \\ 0 \\ 0 \end{bmatrix}$$

For further simplification we write:

$$\begin{bmatrix} A_{11} & 0 & A_{13} & 0 \\ 0 & A_{22} & 0 & A_{24} \\ A_{31} & A_{32} & A_{33} & A_{34} \\ A_{41} & A_{42} & A_{43} & A_{44} \end{bmatrix} \cdot \begin{bmatrix} C_E \\ C_H \\ D_E \\ D_H \end{bmatrix} = \begin{bmatrix} 0 \\ 0 \\ 0 \\ 0 \end{bmatrix}$$

The determinant is expanded and set to zero

$$A_{11} \cdot \begin{bmatrix} A_{22} & 0 & A_{24} \\ A_{32} & A_{33} & A_{34} \\ A_{42} & A_{43} & A_{44} \end{bmatrix} + A_{31} \cdot \begin{bmatrix} 0 & A_{13} & 0 \\ A_{22} & 0 & A_{24} \\ A_{42} & A_{43} & A_{44} \end{bmatrix} - A_{41} \cdot \begin{bmatrix} 0 & A_{13} & 0 \\ A_{22} & 0 & A_{24} \\ A_{32} & A_{33} & A_{34} \end{bmatrix} = 0$$

$$A_{11}A_{22} \cdot \begin{bmatrix} A_{33} & A_{34} \\ A_{43} & A_{44} \end{bmatrix} - A_{11}A_{32} \cdot \begin{bmatrix} 0 & A_{24} \\ A_{43} & A_{44} \end{bmatrix} + A_{11}A_{42} \cdot \begin{bmatrix} 0 & A_{24} \\ A_{33} & A_{34} \end{bmatrix}$$

$$-A_{31}A_{22} \cdot \begin{bmatrix} A_{13} & 0 \\ A_{43} & A_{44} \end{bmatrix} + A_{31}A_{42} \cdot \begin{bmatrix} A_{13} & 0 \\ 0 & A_{24} \end{bmatrix}$$

$$+A_{41}A_{22} \cdot \begin{bmatrix} A_{13} & 0 \\ A_{33} & A_{34} \end{bmatrix} - A_{41}A_{32} \cdot \begin{bmatrix} A_{13} & 0 \\ 0 & A_{24} \end{bmatrix} = 0$$

and finally we get :

$$A_{11}A_{22}A_{33}A_{44} - A_{11}A_{22}A_{34}A_{43} + A_{11}A_{32}A_{24}A_{43} - A_{11}A_{42}A_{33}A_{24}$$
$$-A_{31}A_{22}A_{13}A_{44} + A_{31}A_{42}A_{13}A_{24} + A_{41}A_{22}A_{13}A_{34} - A_{41}A_{32}A_{13}A_{24} = 0$$

Re-substitution leads to:

$$-J_p^2K_p^2\frac{p^2\beta^2a^2}{\mathrm{v}^4}+J_p^2K_p'^2\frac{\mu_0\varepsilon_0\omega^2a^4n_m^2}{\mathrm{v}^4}+J_pJ_p'K_pK_p'\frac{\mu_0\varepsilon_0\omega^2a^4n_m^2}{u^2\mathrm{v}^2}-J_p^2K_p^2\frac{p^2\beta^2a^3}{u^2\mathrm{v}^2}$$
$$-J_p^2K_p^2\frac{p^2\beta^2a^3}{u^2\mathrm{v}^2}-J_p^2K_p^2\frac{p^2\beta^2a^3}{u^4}+J_pJ_p'K_pK_p'\frac{\mu_0\varepsilon_0\omega^2a^4n_k^2}{\mathrm{v}^2u^2}+\frac{\mu_0\varepsilon_0\omega^2a^4n_k^2}{u^4}J_p'^2K_p^2=0$$
$$\frac{J_p'^2}{J_p^2}\frac{\mu_0\varepsilon_0\omega^2a^4n_k^2}{u^4}+\frac{K_p'^2}{K_p^2}\frac{\mu_0\varepsilon_0\omega^2a^4n_m^2}{\mathrm{v}^4}+\frac{J_pJ_p'K_pK_p'}{J_p^2K_p^2}\left(\frac{\mu_0\varepsilon_0\omega^2a^4n_m^2}{u^2\mathrm{v}^2}+\frac{\mu_0\varepsilon_0\omega^2a^4n_k^2}{u^2\mathrm{v}^2}\right)$$
$$-\frac{p^2\beta^2a^2}{\mathrm{u}^4}-\frac{p^2\beta^2a^2}{u^2\mathrm{v}^2}-\frac{p^2\beta^2a^3}{u^2\mathrm{v}^2}-\frac{p^2\beta^2a^2}{\mathrm{v}^4}=0$$

Collecting terms:

$$\frac{J_p'^2}{J_p^2}\frac{n_k^2}{u^4}+\frac{K_p'^2}{K_p^2}\frac{n_m^2}{\mathrm{v}^4}+\frac{J_pJ_p'K_pK_p'}{J_p^2K_p^2}\left(\frac{n_m^2}{u^2\mathrm{v}^2}+\frac{n_k^2}{u^2\mathrm{v}^2}\right)-\frac{p^2\beta^2}{\mu_0\varepsilon_0\omega^2a^2}\left(\frac{1}{\mathrm{u}^4}+\frac{2}{u^2\mathrm{v}^2}+\frac{1}{\mathrm{v}^4}\right)=0$$

Rewriting:

$$\frac{J_p'^2}{J_p^2}\frac{n_k^2}{u^4}+\frac{K_p'^2}{K_p^2}\frac{n_m^2}{\mathrm{v}^4}+\frac{J_p'}{J_p}\frac{K_p'}{K_p}\left(\frac{n_m^2}{u^2\mathrm{v}^2}+\frac{n_k^2}{u^2\mathrm{v}^2}\right)-\frac{p^2\beta^2}{\mu_0\varepsilon_0\omega^2a^2}\left(\frac{\mathrm{u}^2+\mathrm{v}^2}{u^2\mathrm{v}^2}\right)^2=0$$

Carrying out the differentiation with respect to *r* and redefinition:

$$J_p'(k_k\cdot r)=\frac{\partial J_p\left(k_k\cdot r\right)}{\partial r}=k_k\frac{\partial J_p(u)}{\partial u}=k_k\cdot J_p'\left(u\right)$$
$$K_p'(ik_k\cdot r)=\frac{\partial K_p\left(ik_k\cdot r\right)}{\partial r}=ik_m\frac{\partial K_p(\mathrm{v})}{\partial \mathrm{u}}=ik_m\cdot K_p'\left(\mathrm{v}\right)$$

we get:

$$\frac{k_k^2J_p'^2(u)}{J_p^2}\frac{n_k^2}{u^4}-\frac{k_m^2K_p'^2(\mathrm{v})}{K_p^2}\frac{n_m^2}{\mathrm{v}^4}+\frac{k_kJ_p'(u)}{J_pu^2}\frac{ik_mK_p'(\mathrm{v})}{K_p\mathrm{v}^2}\left(n_m^2+n_k^2\right)-\frac{p^2\beta^2}{\mu_0\varepsilon_0\omega^2a^2}\left(\frac{\mathrm{u}^2+\mathrm{v}^2}{\mathrm{u}^2\mathrm{v}^2}\right)^2=0$$

$$\frac{J_p'^2(u)}{u^2J_p^2}n_k^2+\frac{K_p'^2(\mathrm{v})}{\mathrm{v}^2K_p^2}n_m^2+\frac{J_p'(u)}{uJ_p}\frac{K_p'(\mathrm{v})}{\mathrm{v}K_p}\left(n_m^2+n_k^2\right)-\frac{p^2\beta^2}{\mu_0\varepsilon_0\omega^2}\left(\frac{\mathrm{u}^2+\mathrm{v}^2}{\mathrm{u}^2\mathrm{v}^2}\right)^2=0$$

By using the abbreviation for:

$$X_p=\frac{J_p'(u)}{uJ_p(u)}k_k;X_p=\frac{K_p'(\mathrm{v})}{\mathrm{v}K_p(\mathrm{v})}ik_m\ ;\omega=c\cdot k;c=\frac{1}{\sqrt{\mu_0e_0}}$$

$$Y_p^2n_k^2+X_p^2n_m^2+Y_pX_p\left(n_m^2+n_k^2\right)-\frac{p^2\beta^2}{k^2}\left(\frac{u^2+\mathrm{v}^2}{u^2\mathrm{v}^2}\right)^2=0$$

we get:

$$Y_p=-X_p\frac{n_m^2+n_k^2}{2n_k^2}\pm\sqrt{\left(\frac{n_m^2+n_k^2}{2n_k^2}X_p\right)^2-X_p^2\frac{n_m^2}{n_k^2}-\frac{p^2\beta^2}{n_k^2k^2}\left(\frac{u^2+\mathrm{v}^2}{u^2\mathrm{v}^2}\right)^2}$$

With rewriting the square root:

$$\left(\frac{n_m^2+n_k^2}{2n_k^2}\right)^2 X_p^2-\frac{n_m^2}{n_k^2}X_p^2=\frac{X_p^2}{n_k^2}\left(\frac{\left(n_m^2+n_k^2\right)^2-4n_k^2n_m^2}{4n_k^2}\right)=\left(\frac{n_k^2-n_m^2}{2n_k^2}X_p\right)^2$$

we finally get

$$Y_p=-X_p\frac{n_m^2+n_k^2}{2n_k^2}\pm\sqrt{\left(\frac{n_k^2-n_m^2}{2n_k^2}X_p\right)^2-\frac{p^2\beta^2}{n_k^2k^2}\left(\frac{u^2+\mathrm{v}^2}{u^2\mathrm{v}^2}\right)^2}$$

Let's rewrite Y_p again as J_p and let's use the derivation of the Bessel-function with respect to its argument:

$$Y_p=\frac{J_p'(u)}{uJ_p(u)}=\frac{1}{uJ_p(u)}\frac{\partial J_p(u)}{\partial u}=\frac{1}{uJ_p(u)}\left(\mp\frac{p}{u}J_p(u)\pm J_{p\mp1}(u)\right)=\pm\frac{J_{p\mp1}(u)}{uJ_p(u)}\mp\frac{p}{u^2},$$

so we get:

$$\frac{J_{p-1}(u)}{J_p(u)}=-\frac{n_m^2+n_k^2}{2n_k^2}uX_p+\left\{\frac{p}{u}-u\sqrt{\left(\frac{n_k^2-n_m^2}{2n_k^2}X_p\right)^2-\frac{p^2\beta^2}{n_k^2k^2}\left(\frac{u^2+\mathrm{v}^2}{u^2\mathrm{v}^2}\right)^2}\right\}$$

$$\frac{J_{p+1}(u)}{J_p(u)}=\frac{n_m^2+n_k^2}{2n_k^2}uX_p+\left\{\frac{p}{u}-u\sqrt{\left(\frac{n_k^2-n_m^2}{2n_k^2}X_p\right)^2-\frac{p^2\beta^2}{n_k^2k^2}\left(\frac{u^2+\mathrm{v}^2}{u^2\mathrm{v}^2}\right)^2}\right\}$$

Using for the coefficient of propagation β the relation (2.5.12),

$$\frac{\beta^2-k^2n_m^2}{k^2\left(n_k^2-n_m^2\right)}=\frac{\mathrm{v}^2}{u^2+\mathrm{v}^2}\Rightarrow\beta^2=\frac{\mathrm{v}^2k^2\left(n_k^2-n_m^2\right)}{u^2+\mathrm{v}^2}+k^2n_m^2$$

we get the solution :

$$\frac{J_{p+1}(u)}{J_p(u)}=\frac{n_m^2+n_k^2}{2n_k^2}uX_p+\left\{\frac{p}{u}-u\sqrt{\left(\frac{n_k^2-n_m^2}{2n_k^2}X_p\right)^2-p^2\left(\frac{1}{u^4}+\frac{1}{\mathrm{v}^2}\right)\cdot\left(\frac{n_m^2}{n_k^2}\frac{1}{\mathrm{v}^4}+\frac{1}{u^2}\right)}\right\} \qquad \textbf{(7.2.1)}$$

$$\frac{J_{p-1}(u)}{J_p(u)}=-\frac{n_m^2+n_k^2}{2n_k^2}uX_p+\left\{\frac{p}{u}-u\sqrt{\left(\frac{n_k^2-n_m^2}{2n_k^2}X_p\right)^2-p^2\left(\frac{1}{u^4}+\frac{1}{\mathrm{v}^2}\right)\cdot\left(\frac{n_m^2}{n_k^2}\frac{1}{\mathrm{v}^4}+\frac{1}{u^2}\right)}\right\} \qquad \textbf{(7.2.2)}$$

8 Laser safety

8.1 Laser safety remarks

The EXP12 experimental set-up contains a laser which is only suitable for laboratory applications.
With the individual modules in the assembled state, laser radiation (semiconductor laser) can be produced at 805 nm with a maximum power of 50 mW.

The complete assembled laser is therefore a product which exhibits the power characteristics of a Class 3B laser.

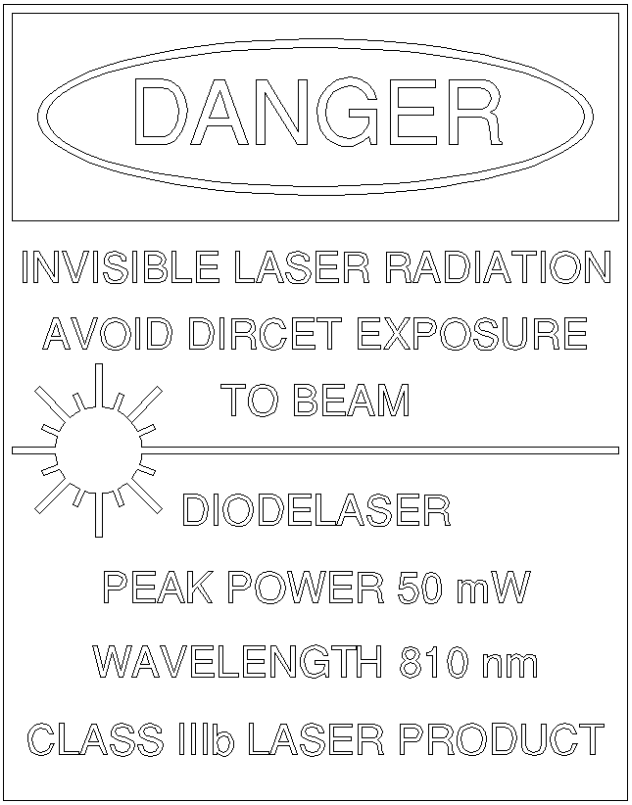

The user must observe the laser safety regulations, e.g.

DIN VDE 0837 or IEC 0837.

In these guidelines of February 1986 the following points are listed for the operation of laser equipment in laboratories and places of work.

Laser equipment in laboratories and places of work

Class 3B laser equipment

Class 3B lasers are potentially hazardous, because a direct beam or a beam reflected by a mirror can enter the unprotected eye (direct viewing into the beam). The following precautions should be made to prevent direct viewing into the beam and to avoid uncontrolled reflections from mirrors:

a.) The laser should only be operated in a supervised laser area

b.) Special care should be taken to avoid unintentional reflections from mirrors

c.) Where possible the laser beam should terminate on a material which scatters the light diffusely after the beam has passed along its intended path. The colour and reflection properties of the material should enable the beam to be diffused, so keeping the hazards due to reflection as low as possible.

Note: Conditions for safely observing a diffuse reflection of a Class 3B laser which emits in the visible range are : Minimum distance of 13 cm between screen and cornea of the eye and a maximum observation time of 10s. Other observation conditions require comparison of the radiation density of the diffused reflection with the MZB value.

d.) Eye protection is necessary if there is a possibility of either direct or reflected radiation entering the eye or diffuse reflections can be seen which do not fulfil the conditions in c.).

e.) The entrances to supervised laser areas should be identified with the laser warning symbol

MZB means Maximum Permissible Radiation (Maximal zulässige Bestrahlung) and it is defined in section 13 of DIN/VDE 0837.

Special attention is drawn to point 12.4 of DIN VDE0837:

Laser equipment for demonstration, display and exhibition purposes

Only Class 1 and Class 2 lasers should be used for demonstrations, displays and exhibitions in unsupervised areas.

Lasers of a higher class should then only be permitted if the operation of the laser is controlled by an experienced and well trained operator and/or the spectators are protected from radiation exposure values which does not exceed the applicable MZB values.

Each laser system, which is used in schools for training etc. should fulfil all the applicable requirements placed on class 1 and class 2 laser equipment; also, it should not grant persons access to radiation which exceeds the applicable limits in Class 1 or Class 2.

9 Laser Diode Controller LDC-01

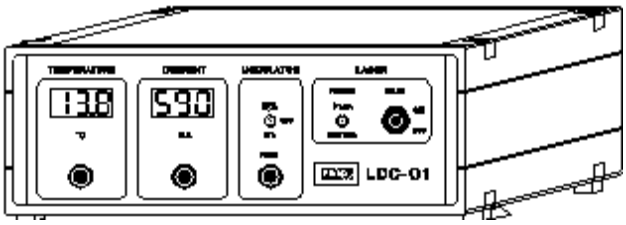

9.1 Technical specifications LDC-01

Temperature Controller:

Controlling Range	10 to 40 °C
Accuracy	± 0.1 °C
Time of Response	10 to 30 sec
Max. Current for TEC	1000 mA

Current Controller:

Controlling Range, max. is set by manufacturer to the used laserdiode	0 - 1000 mA
Accuracy	± 1 mA

Internal Modulator:

for modulating the injection current

Amplitude, max. is set by manufacturer to the used laserdiode	0 - 1000 mA rectangular
Rise Time	1 µsec
Modulation Frequency	0.5 - 60 Khz

Internal Modulation Amplifier:

for use of an external modulation source

Input Amplitude	0 - 5 Volt
Cut-Off Frequency	1 MHz

Photodiode Amplifier:

Input Impedance	
50 Ohm	
Gain	1 - 100 selectable

Monitor Signals:

Temperature	100 mV / °C
Injection Current	5 mV / mA
Modulator Synchronisation signal	TTL

The Temperature controller section

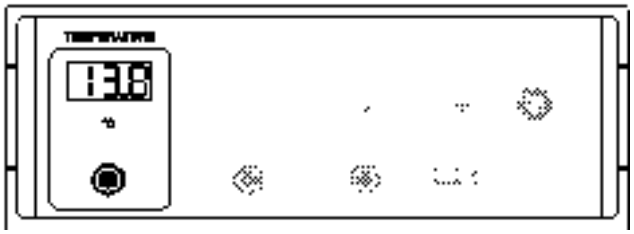

Fig. 50 : Front panel temperature display and setting

The actual temperature of the laserdiode crystal is displayed on the LED panel in °C. The desired value of the temperature is set by the knob of a 5 turn potentiometer. The controller needs a setting up time of about 10-30 sec. The accuracy of stabilisation amounts ± 0.1 °C.

The Injection current section

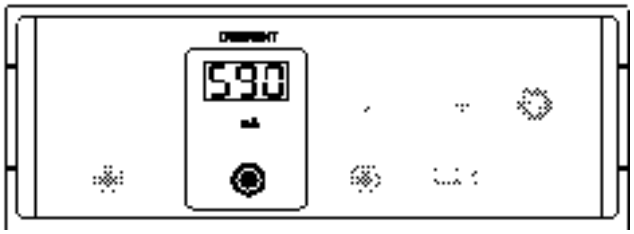

Fig. 51 : Front panel injection current display and setting
The actual value of the current of the laserdiode, also termed injection current, is displayed in mA on the LED panel. The desired value can be set by the 5 turn potentiometer and is stabilised within ± 1 mA. Please note that the setting is only active when the modulator switch (see Fig. 52) is set to the "**OFF**" Position.

The Modulator

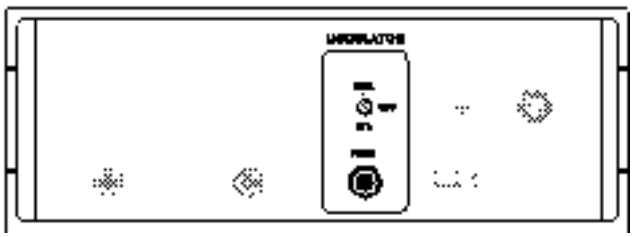

Fig. 52 : Front panel modulator settings
The front panel switch can be set to three positions. In the "**INT**" position the injection current is internally switched on and off to the pre-set current which is set by the "**mA**" knob. The switching frequency can be set by the knob "**FREQ.**" in a range from 0.5 - 60 kHz. The rise and fall time amounts to 1 µsec. When the front panel switch is set to "**EXT.**" the current can be modulated by means of an external source which is connected to the "**EXT. MOD.**" input at the rear panel (see Fig. 55).

The Laser Main Switches

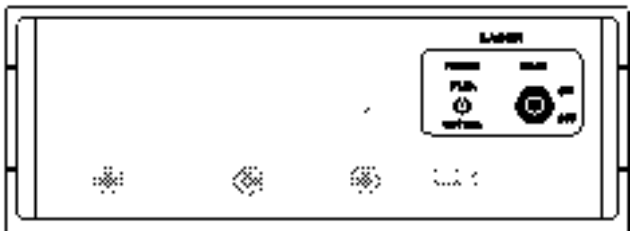

Fig. 53 Front panel laser switches

To fulfil the laser safety regulations the LDC01 is supplied with a key switch. This key only switches the laser current off.

Important note:
To ensure the longest possible life-time of the laserdiode it is highly recommended only to use the key switch "**HEAD**" when the injection current is set to its lowest level. This should also be obeyed for the use of the "**POWER**" switch. When the "**HEAD**" key switch is in the "**ON**" position the red LED located at the backside of the laserhead is powered on to indicate that laser emission can occur.

The OUTPUTS at the Rear Panel

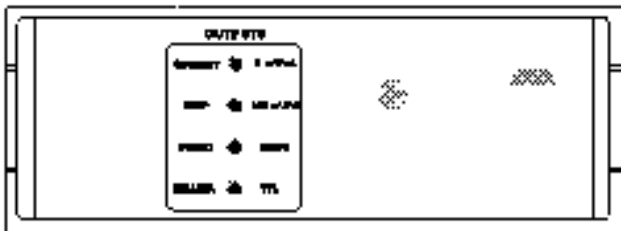

Fig. 54 : BNC output sockets at the rear panel

For external monitoring the following signals are provided via BNC sockets:

"**CURRENT**"	monitor signal set to 5 mV / mA.
"**TEMP**"	monitor signal set to 100 mV/°C.
"**PHOTO DIODE**"	this output is connected to the internal photo detector amplifier see (Fig. 60)
"**INT.MOD**"	monitor signal of the int. modulator set to TTL level.

The "INPUTS" at the rear panel

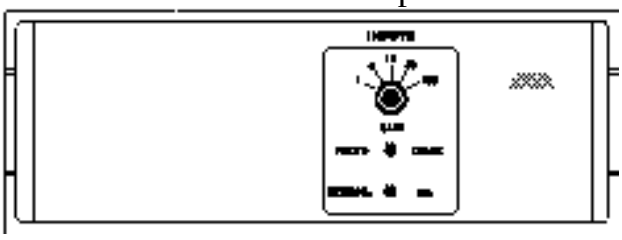

Fig. 55 : BNC input sockets at the rear panel
The LDC01 is supplied with a fast amplifier in connection with the photodiode Module G of the experimental set-up. The input "**PHOTO DIODE**" has a low impedance of 50 Ω and is amplified by a factor set with the "**GAIN**" knob. The input assigned "**EXT. MOD.**" allows the connection of an external modulating source. The input is DC coupled and the signal of the external source must be positive in a range from 0 to 5 Volts.

The Connection of the Laserhead

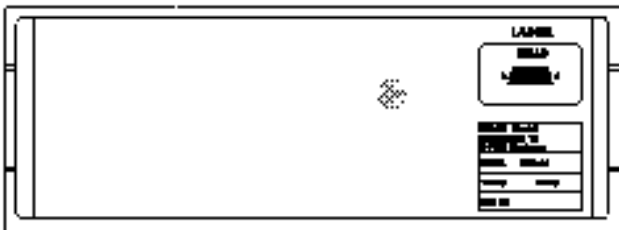

Fig. 56 : The laserhead connector
The laserhead containing the laserdiode with its TEC, and temperature sensor is connected with a so called 15 pin VGA connector to the controller unit LDC01. The fixing screws of the connector are sealed. Each laserdiode, especially the high power types, has individual characteristics concerning mainly the sensitivity of the power monitor diode. So the internal control loops have to be matched to each diode. Another aspect is the danger of destroying the expensive laserdiode when interrupting the connection with powered laserdiode. Please understand that no guaranty can be granted by a broken seal.

The Mains Supply

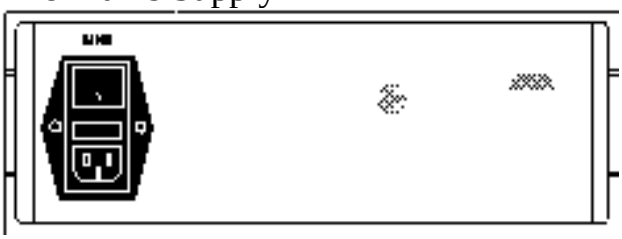

Fig. 57 : Mains supply connector
The fully integrated mains supply connector contains the mains switch, a fuse (250 mA medium inert) as well a spare fuse. The mains line voltage must be 230 Volts AC ± 10%. The power consumption of the LDC01 amounts to 60 VA.